Evaluating the Ethical Decision-Making of ASL Interpreters

Maggie Zuvich
Bloomsburg University of Pennsylvania

INTRODUCTION

American Sign Language Interpreting is a relatively new profession, not established formally until 1964. As the field rapidly evolves, so do the models that guide interpreters' ethical decision-making. The interpreter models, or the way an interpreter views her role and responsibilities, are an important framework for understanding how and why interpreters make the decisions they do. For example, the helper model is a perspective often considered problematic, as it can lead interpreters to pity Deaf people and treat them as incapable of living independently. The conduit model was born in direct response to the helper model, instead viewing the interpreter as a machine, a 9-to-5 worker who does not interact with the Deaf community outside of interpreting for them. The communication facilitation model was created in response to the conduit model and encouraged interpreters to begin advocating for themselves, prioritizing their needs as a professional as well as the needs of the Deaf consumers. The bilingual-bicultural model expanded on this model, emphasizing cultural mediation that results in improved dynamic equivalence. The ally model encourages hearing interpreters to understand the power imbalance between themselves and their Deaf consumers, and to make interpreting decisions within current social and political contexts.

> ***Key Finding: Prioritization of Personal Morality***
> *"When I finished working with students, I have hosted, at home, private video calls with a hearing girl and a Deaf boy who were trying to socialize at school, and I'm like, 'I'll pop on for the first couple calls, get you started, teach her some signs, and then you guys are on your own.' I've done that. Ethical? I don't know. It just seems right."*

Though newer models are now taught in interpreter education programs, some interpreters move between models, even the older models. Though these models were typically considered oppressive, their use in certain situations may be useful if executed appropriately. The use of the interpreter models, in addition to many other factors, impact the way an interpreter facilitates communication, how she views the power dynamic between her and a client, how she views the relationship between her and a client, and how she sets or even crosses boundaries. This study examines the many factors that impact an interpreter's ethical decision-making. As the field evolves and expands, so must the ethical and professional standards to which interpreters should be held. A limited supply of interpreters often forces Deaf consumers to settle for inadequate interpreters, whether that inadequacy comes from a lack of skill or a lack of appropriate ethical and professional standards. While this research does not find interpreters to be overtly unethical and unprofessional, it becomes clear how important it is to have these nuanced discussions.

STUDY AIMS

1. To understand how interpreters view their role and the power dynamic between themselves and their clients.
2. To analyze the influences on an interpreter's ethics, boundaries, and decision-making.
3. To explore how interpreters move between and use different interpreting models.

LITERATURE REVIEW

Perhaps because it is a relatively new profession, there is little literature on the practice of interpreting. As a result, literature on ethical issues in other professions served as a starting point for this project.

Power Dynamics Between Professional and Client

The sometimes glaring power imbalances that exist between professionals and their clients often must be addressed for successful interactions between both parties (Borges and Goodman 2020). Working with a marginalized or vulnerable population requires a significant amount of responsibility and accountability. The way professionals understand and conceptualize their role and responsibilities differ on an individual basis, meaning their ethical boundaries and decisions are not solely based on those established by the governing body of their industry, but by their own personal morals and values.

LITERATURE REVIEW (continued)

Ethical Boundaries Set by a Governing Body vs. Personal Morality

Ethical standards established by an industry's governing body commonly act as guidelines that are understood objectively by individual professionals. Even if there seems to be clear guidance on a particular scenario, professionals may hesitate to follow that guidance if they notice new, unexpected factors in any given situation, instead acting based on "what one feels is right" (Forsner et al. 2020). Personal values and beliefs are obviously critical to ethical decision-making.

Lack of Sufficient Training

In fact, across each of the studies in this literature review, because of the subjective nature of ethics and ethical decision-making, many feel that professionals, especially newer professionals, need a stronger foundation from their ethics training. In each of these studies, professionals are often put in high-stress, high-stakes scenarios that tax or strain personal morality or responsibility.

> ***Key Finding: Creating and Following Boundaries***
> *"We've had students come crying to us in the office, I get it – we know their language. But we also know where our limitations are."*

There are clearly stones left unturned in ethical trainings. No complicated ethical scenario has an easy solution – or even one solution at that – but it becomes clear through these studies that professionals feel insufficiently supported in their ethical trainings. Interpreting is an occupation with unique ethical challenges, including the complicated power dynamic between hearing interpreter and Deaf client, the difficulty of defining clear boundaries, and the insufficient training that often does not adequately address these challenges.

METHODS

Over a span of about a month, nine individual interviews were conducted with hearing interpreters, regardless of their years of experience, certification status, or otherwise; the only necessary factor was that the participant must currently be working as an ASL/English interpreter. All nine participants were women, with seven white and two Black participants. All but two interpreters live and work in the state of Pennsylvania; the remaining two live in Delaware, which has very different standards and qualifications for their interpreters. Both work primarily in Delaware, though one of the two also works in surrounding states. Years of experience ranged from 10 months to almost 30 years. Snowball sampling was used to recruit participants, though most contacts were already known to the researcher through previous observations or interactions. Interviews were semi-structured, using both a predetermined set of questions and unplanned prompts that encouraged participants to expand on their answers. The transcripts of each interview are being coded using Atlas.ti, a qualitative analysis software, using an inductive approach to analysis. Data analysis is still in its early stages and has not yet been completed; the results of this study, therefore, reflect only a small portion of the data set.

> ***Key Finding: Perception of Power Imbalances***
> *"Yes, there's a power imbalance. I would say almost instinctively, in my opinion…I feel like the interpreter is almost assumed all the power in the room…whether you want it or not."*

RESULTS

Data analysis is still in its early stages; therefore, only a small fraction of the data set is reflected in the following results.

> ***Key Finding: Creating and Following Boundaries***
> *I tried to explain to them what the role of the interpreter is, and it's very difficult when they say another interpreter does it, another interpreter does that. You have to know for yourself what those boundaries are, and you have to stay true to them.*

Conceptualization of Role

While all interpreters generally view communication facilitation as their primary role as an interpreter, the behaviors and responsibilities beyond doing the actual, physical act of interpreting depend on the interpreter. Younger, or, more accurately, newer, interpreters see their role as an ally to the Deaf consumer and the Deaf community. Those who rely on the ally model typically have more of a hands-on approach to interpreting, especially if interpreting for children in an educational setting. For example, one interpreter shared that she interpreted (free of charge) several video calls between a hearing and Deaf student after school hours to help teach signs to the hearing student and make it easier for the two to communicate independently. The interpreter admitted that she didn't know if it was technically ethical, but "it just seem[ed] right."

RESULTS (continued)

Perception of Power Imbalance

All interpreters also technically recognized a power imbalance between themselves and their Deaf consumers, though that understanding of the power dynamics varied among interpreters. Some found the power imbalance relatively inconsequential and easy to address, such as this interpreter, who states, "At times, yes…I have more information, which is power. And I often tell the Deaf person what I know, you know?" Interpreters instead discussed at length the power imbalances between the Deaf and hearing consumers much more.

Influences on Ethical Standards and Decision-Making

An interpreter's understanding of power dynamics and ethical standards are about as unique as each individual interpreter. Interpreters agree that their education provided a solid foundation for their ethical standards, and experience in the field helped flesh out those standards. Some also refer directly to their own personal morals and values that help guide their decision-making. One interpreter referenced her spirituality as a strong influence on her interpreting. When asked how it affects the decisions she makes, she responded, "Everything that's important to us influences our decision-making, you know, so, it does, it does. It does impact my decision making, as far as like, how I see people. Or the fact that I do see people…people are just important to me. And I think they're important to me because I'm taught that they're important to God, you know? And I'm taught that they are my brothers and sisters, and if you can help, you know, help!"

> ***Key Finding: Use of Interpreting Models***
> *"Because it really depends – I really feel like any of [the models] can be at play at some point in your interpreting life."*

Use of Interpreting Models

Interpreters had a loose understanding of or familiarity with the interpreting models, and were able to connect with at least one of the models more than the others. For example, one interpreter said she "naturally" fit the helper model, while another found the communication facilitator model closer to her interpreting style. The interpreter who connected more with the helper model seemed to have a much more hands-on approach to interpreting, especially in an educational setting, while the interpreter who connected most to the communication facilitator model seemed to set much clearer boundaries, again within the educational setting. While all agreed that any of the models could be useful at any time (including some of the older models that are typically seen as more oppressive), the one that best fit an interpreter's interpreting style seemed to reflect their decision-making, how they viewed their relationships with their consumers, and, likewise, the boundaries (or lack thereof) that they set with those consumers.

CONCLUSIONS

This study delves deeper into the broad subject of ethical decision-making. Results suggest that while ethics are subjective for a multitude of reasons, an interpreter's decision-making and how she sets and/or crosses boundaries may relate to the interpreting model she most closely connects and relates to.

REFERENCES

Borges, A.M., & Goodman, L.A. (2020). Considering poverty in the therapeutic process: Experienced therapists' adaptations. *Counseling Psychology Quarterly, 33*(4). 490-515. https://doi.org/10.1080/09515070.2019.1582457

Forsner, M., Elvhage, G., Ewalds-Kvist, B.M., & Lützén, K. (2020). Moral challenges when suspecting abuse and neglect in school children: A mixed method study. *Child and Adolescent Social Work Journal, 38*. 599-610. https://doi.org/10.1007/s10560-020-00680-4

McMillan, Lesley. (2018). Police officers' perceptions of false allegations of rape. *Journal of Gender Studies, 27*(1). 9-21. https://doi.org/10.1080/09589236.2016.1194260

Russell, D. & Shaw, R. (2016). Power and privilege: An exploration of decision-making of interpreters. *Journal of Interpretation, 1*(7), 1-26.

Data Quality Differs by Race and Ethnicity: Evidence from CPS for Black Hispanics

Jingyi Zhou, Advised by Professor Stephan Lefebvre
Department of Economics, Bucknell University, Lewisburg PA

Research Question

How do **sample size** and **survey methodology** of the CPS (Current Population Survey) impact the **population statistics estimators** (standard errors and confidence intervals) of **racial/ethnic minority groups**, in particular the Black Hispanic group?

Background

- The **Current Population Survey** is a monthly survey of 50,000–60,000 households conducted by the Census Bureau. It is one of the oldest, largest, and most well-recognized surveys in the US. It provides important information on **individuals and families,** including education, work, and earnings data.
- In **statistical estimation**, our confidence in that estimate is represented by the margin of error which can be represented as a confidence interval (CI). A smaller CI indicates a more precise estimation.
- **Race** is a complex social phenomena. The goal of data collection around race and ethnicity is to produce a fuller understanding of racialization as a social process. The idea of an objective standard for measuring race, for example, is no longer tenable in social science research.
- In most publicly administered surveys, **Black Hispanics** are counted as individuals who identify as both Black and as Hispanic. They may be Afro-Hispanic, mixed race, or they may have some other reason for choosing these identities.

Importance

Research indicates that **both race and ethnicity** shape economic life in the US. Publicly available data that is high quality, timely, and accurate is vital to monitor and study social inequality in the US. Many researchers use the CPS and consider it to be the gold standard for studying labor market and demographic trends nationally. The goal of this study is to **quantify the uncertainty around point estimates of important economic concepts (average income, unemployment rate) for Black Hispanics**. This group is of particular interest because, to understand racialization in the US, we must attend to the color line within the Hispanic community.

Research Process

1. Explore Research Question & Data
Learn about CPS survey methodologies and questionnaire design. Compare different data extracting platforms, such as CEPR and IPUMS.

2. Download & Clean the Survey Data
Benchmarking with published statistics of CPS (i.e. compare statistics that you calculate with published statistics using the same data).

3. Generate Summary Statistics
Apply **survey weight** and **SDR** (Successive Difference Replication) to the sample using 160 replicate weights. This helps to generate empirically derived standard error estimates which are more precise than single weight estimates
[Stata code]: *svyset [iw=asecwt], sdrweight(repwtp1-repwtp160) vce(sdr) mse*

4. Observe & Summarize
Compare summary statistics across racial/ethnic groups, compare with other data sources, create **visualized graphs and diagrams**, draw **real world connections** from results.

Results

Figure 1: Sample Size & Population Size (weighted) by Race & Ethnicity in Comparison with Census

Race	2018 CPS ASEC				2020 Census	
	Sample Size	% of Total	Weighted Size	% of Total	Census Size	% of Total
White Only	138,178	76.7%	247,695,200	76.6%	204,277,273	61.6%
Black Only	21,857	12.1%	42,563,790	13.2%	41,104,200	12.4%
Asian Only	11,226	6.2%	19,483,630	6.0%	19,886,049	6.0%
Others	8,823	5%	13,413,480	4.2%	66,181,759	20.0%
Total	180,084	100.0%	323,156,100	100.0%	331,449,281	100.0%

Ethnicity & Race	2018 CPS ASEC				2020 Census	
	Sample Size	% of Total	Weighted Size	% of Total	Census Size	% of Total
All Hispanic	35,726	19.8%	59,277,160	18.3%	62,080,044	18.7%
White Only Hispanic	32,687	18.2%	52,165,000	16.1%	12,579,626	3.8%
Black Only Hispanic	1,121	0.6%	2,849,611	0.9%	1,163,862	0.4%
Other Hispanic	1,918	1%	4,212,589	1.3%	48,336,556	14.6%
Non-Hispanic	144,358	80.2%	263,928,900	81.7%	269,369,237	81.3%
Total	180,084	100.0%	323,156,100	100.0%	331,449,281	100.0%

Figure 2: Percentage Difference between Sample Size and Population Size in CPS ASEC

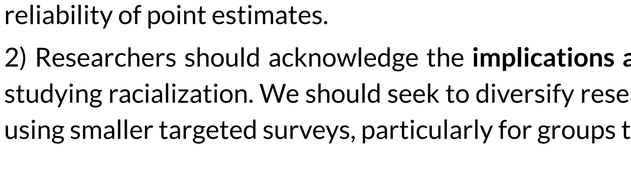

Figure 3: Unemployment Rate with 95% Confidence Intervals by Race & Ethnicity

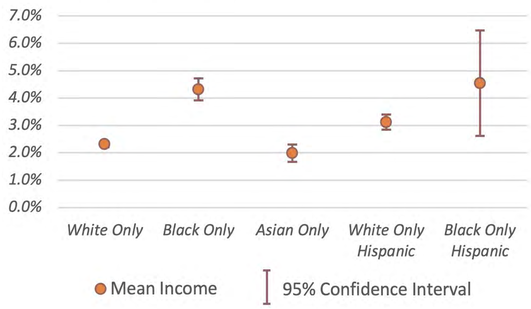

Figure 4: Mean Income and Margin of Error by Race & Ethnicity (dollars)

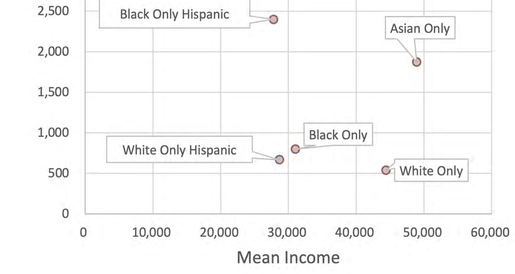

Data Sources: 2018 Current Population Survey (CPS) Annual Social and Economic (ASEC) Supplement, cps.ipums.org, 2020 Census Redistricting Data, census.gov

Main Takeaways

- **Figure 1 & 2:** The proportion of the population that is Black & Hispanic is **50% higher** than this group's proportion in the CPS, while other groups are overrepresented or closer to parity.
- **Figure 3:** The unemployment rate for the Black and Hispanic group has a **larger 95% confidence interval** (from **2.6 to 6.5 percent** unemployment) compared to other ethnic/racial groups.
- **Figure 4:** The Black and Hispanic group has the **lowest mean income** and the **largest margin of error** among comparable groups.

Conclusion

Data quality varies significantly based on race and ethnicity using the CPS. My research shows larger confidence intervals and margins of error for commonly used measures like average income and unemployment rate. As a consequence:

1) The Census, which administers the CPS, should pursue **alternative survey methods** to increase reliability of point estimates.

2) Researchers should acknowledge the **implications and limitations** of using quantitative surveys for studying racialization. We should seek to diversify research methods, including qualitative methods and using smaller targeted surveys, particularly for groups that are not well represented in national surveys.

S.C.I Coal Township

In coordination with

Bucknell University Botanical Garden Project

Reece Pauling
Department of Environmental Studies & Department of Critical Black Studies, Bucknell University, Lewisburg, PA

This Project is funded by the Ekedahl Fund and Bucknell Center for Sustainability & the Environment

Problem

Problem:
What is the role of Green Initiatives, in particularly Horticulture Therapy, in America's Penal System and how can these initiatives be translated into civic engagement within our community?

What Issues are facing our society today and in which ways can we address such issues?

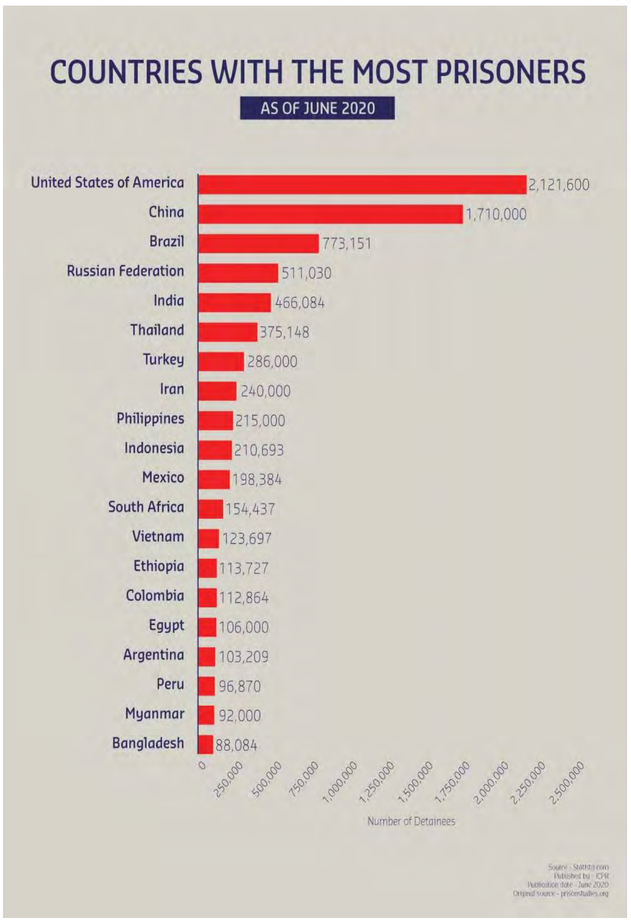

Project Photos

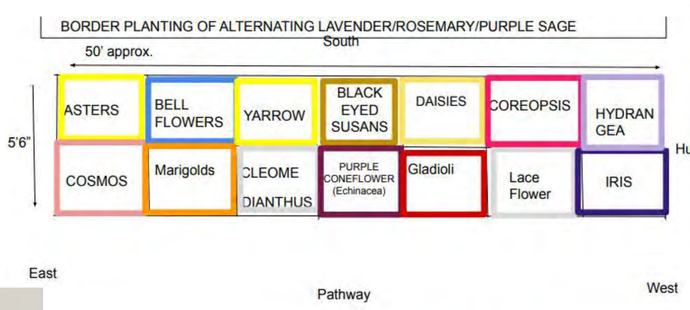

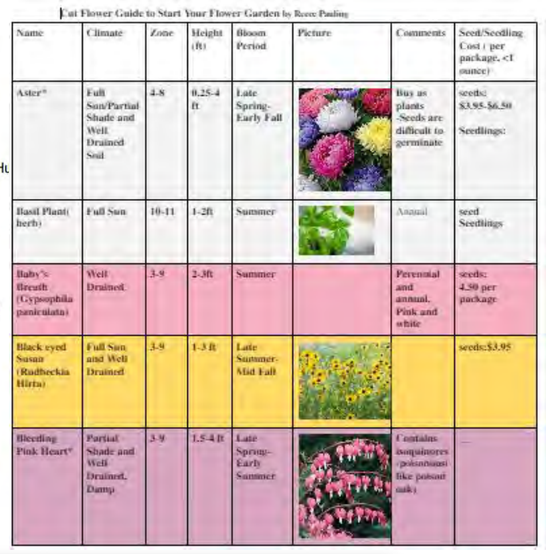
Cut Flower Guide to Start Your Flower Garden by Reece Pauling

Name	Climate	Zone	Height (ft)	Bloom Period	Picture	Comments	Seed/Seedling Cost (per package, <1 ounce)
Aster*	Full Sun/Partial Shade and Well Drained Soil	4-8	0.25-4 ft	Late Spring- Early Fall		Buy as plants -Seeds are difficult to germinate	seeds: $3.95-$6.50 Seedlings:
Basil Plant(herb)	Full Sun	10-11	1-2ft	Summer		Annual	seed Seedlings
Baby's- Breath (Gypsophila paniculata)	Well Drained	3-9	2-3ft	Summer		Perennial and annual, Pink and white	seeds: 4.50 per package
Black eyed Susan (Rudbeckia Hirta)	Full Sun and Well Drained	3-9	1-3 ft	Late Summer- Mid Fall			seeds:$3.95
Bleeding Pink Heart*	Partial Shade and Well Drained, Damp	3-9	1.5-4 ft	Late Spring- Early Summer		Contains isoquinores (poisonous) like poison oak)	

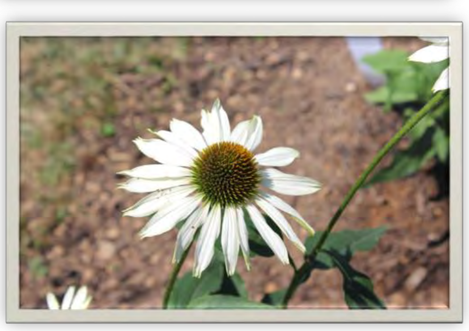

Key Findings

- ❖ According to an annual report from the Pennsylvania Department of Corrections, the three-year recidivism rate in Pennsylvania is 53.4%(World Population Review 2022). The Three year recidivism rate in Northumberland County is 49% (PA DOC Recidivism Report2013).
- ❖ Coal Townships efforts working against punitive state measures
  - Family/Relationship/Self,
  - Sex Offenders Programs
  - Reentry Programs
  - Offense Related Programs
  - Mental Health Programs and Community Work Programs.
  - Academic and Vocational Education Programs

From Horticulture Research

- ❖ 3 types of beneficial Human-nature interactions
  -visible contact
  -presence in nature
  -active participation
- ❖ Building interpersonal Skills
- ❖ Reducing the 8 Criminogenic Needs

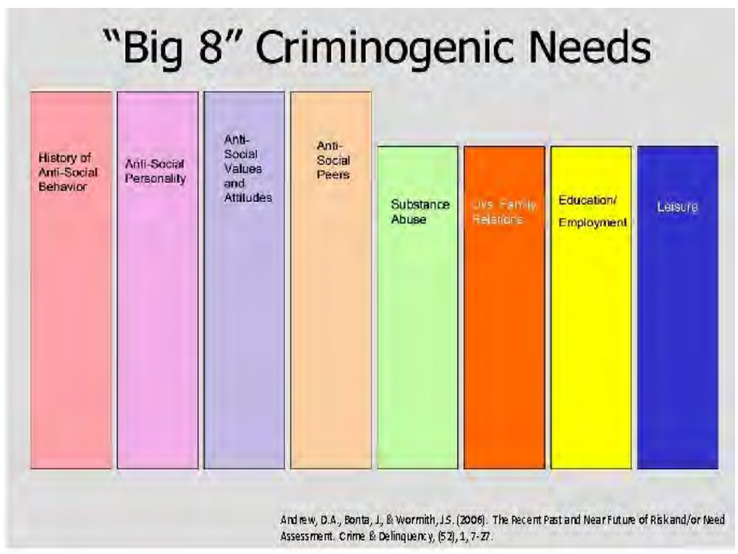

Project Goals

- ❖Create a co-learning experience for Bucknell students and incarcerated individuals
- ❖Foster civic engagement between Community Partners, SCI-Coal Township & Bucknell University
- ❖Contributing to working against punitive state measures through Horticulture Therapy Rehabilitation

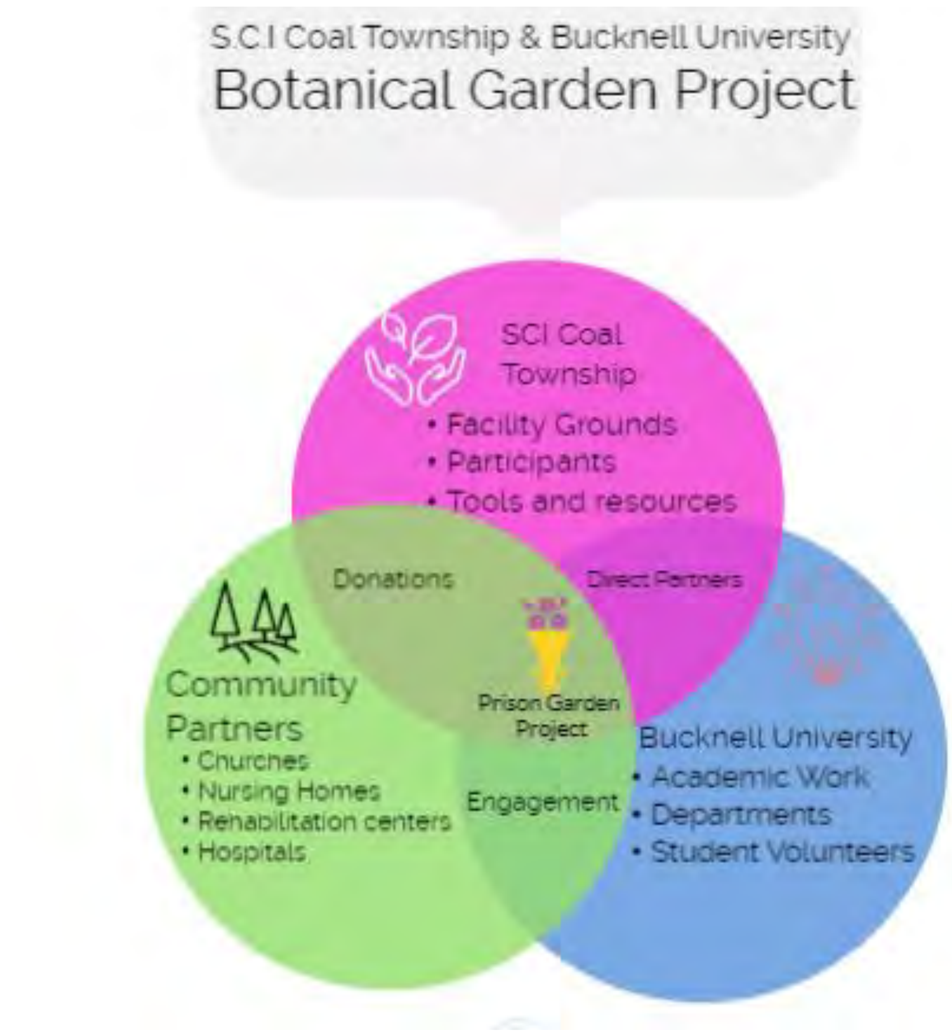

Future Directions

- ❖ Adding to the role of student volunteers
- ❖Growing season pattern for Cut Flowers
- ❖Collecting data on the impacts of the project
- ❖Possibility of adding credentials and vocational training
- ❖Hopes to Cultivate a vegetable garden to combat nutrition and diet in incarcerated individuals

References

World Population Review. (2022). Retrieved July 13, 2022, from https://worldpopulationreview.com/state-rankings/recidivism-rates-by-state

Recidivism report 2013 - Pennsylvania Department of Corrections. (n.d.). Retrieved July 17, 2022, from https://www.cor.pa.gov/About%20Us/Statistics/Documents/Reports/2013%20PA%20DOC%20Recidivism%20Report.pdf

Delaney, R., Subramanian, R., Shames, A., & Turner, N. (2018, October). American history, race, and prison. Retrieved July 7, 2022, from https://www.vera.org/reimagining-prison-web-report/american-history-race-and-prison

Detweiler, M., Sharma, T., Detweiler, J., Murphy, P., Lane, S., Carman, J., . . . Kim, K. (2012, May 22). What is the evidence to support the use of therapeutic gardens for the elderly? Retrieved July 13, 2022, from https://www.ncbi.nlm.nih.gov/pmc/articles/PMC3372556/

Jiang, S., Staloch, K., & Kaljevic, S. (2018). Opportunities and barriers to using hospital gardens ... - jstor home. Retrieved July 14, 2022, from https://www.jstor.org/stable/26598049

Acknowledgements

Mr.Thomas McGinley (Superintendent of SCI Coal Township)
Dr.Katherine Faull (Faculty Mentor)
Stein's Flowers & Gift Inc
Ekedahl Foundation
Community Partners

Stress and Community Identification During COVID-19

Katelyn Bucher & Nick D. Ungson
Susquehanna University

Background

- **Social identity is beneficial for psychological and physical health** [1,2]
  - Social identification satisfies our innate need to belong [3]
  - Increased resilience from social support [4]
- **Identifying with resilient groups is especially important during times of crisis or emergency** [5]
  - People often rally around shared social identities
  - Groups depend on one another to help with emergencies
- **COVID-19 was a unique challenge for social connectedness** [5]
  - Collective identification and social cohesion was hindered
- **Masking rules, social distancing, lockdown mandates** [6]

Hypothesis

Stronger identification with local community will predict lower stress during the COVID-19 pandemic

Method

Participants

American adults recruited using Prolific

Time 1 | April 2020 (*N* = 2500)

Time 2 | October 2020 (*N* = 1106)

Time 3 | March 2021 (*N* = 945)

Local Community Identification (ID)

1 (*strongly disagree*) to 5 (*strongly agree*)

e.g., "I feel a sense of connection to my local community"

e.g., "I am proud to belong to my local community"

e.g., "People who belong to my community trust each other"

Perceived Stress Scale [7]

1 (*never*) to 4 (*very often*)

"In the past two weeks, how often have you...."

e.g., "Been upset because of something that has happened recently"

e.g., "Felt nervous and stressed"

Control Variables

Age, political identification, perceived self-risk, losing income, knowing someone with COVID-19, and essential worker status

Analysis Plan: Regression at 3 time points

Stress ← Local Community ID + Control Variables

Results

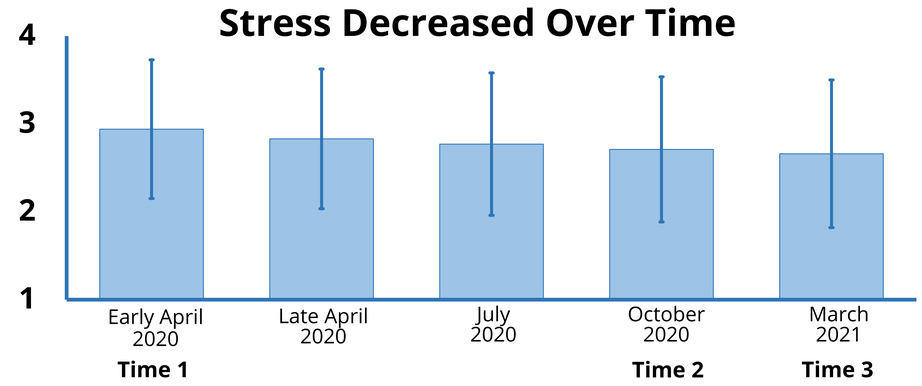

Outcome: Stress

	Time 1	Time 2	Time 3
Local Community ID	**-.19**	**-.16**	**-.15**
Age	**-.14**	**-.01**	**-.02**
Political ID	**-.04**	**-.04**	**-.01**
Perceived self-risk	**.29**	**.23**	.21
Lost income	**.22**	**.23**	**.31**
Knowing someone w/ COVID	**.14**	**.17**	.12
Essential worker	**-.15**		

Bold: $p < .05$

Stronger local community ID predicted lower stress across the COVID-19 pandemic (over and above other control variables like age, political ideology, etc.)

Conclusions & Future Directions

- Support for our hypothesis that **higher identification with local community** predicted less stress during the COVID-19 pandemic
- Although COVID-19 made it difficult for people, those who were able to connect with their local community were less stressed
- **Future Considerations:**
  - Investigating the relationship between identifying with familiar groups (e.g., family) and the relationship it has on stress
  - Does strong local community identification support mask wearing and vaccination practices?

SU Social Identity and Group Processes Lab

Digital Poster and References

Detecting Muscle Fatigue in sEMG Data Through Machine Learning

Allyson K. Clarke[1], Benjamin B. Wheatley[2], Chulhyun Ahn[3]

[1]Department of Biomedical Engineering, Bucknell University, Lewisburg PA
[2]Department of Mechanical Engineering, Bucknell University, Lewisburg PA
[3]Department of Physical Medicine and Rehabilitation, Geisinger, Danville PA

Mechanics and Modeling of Orthopaedic Tissues Lab

Introduction

- Surface electromyography (sEMG) is the electrical reading from muscle stimulation [1] (Figure 1)
- Traditional analyses of sEMG show frequency decreases with muscle fatigue [2]
- There is no simple, universally accepted approach to sEMG fatigue analysis

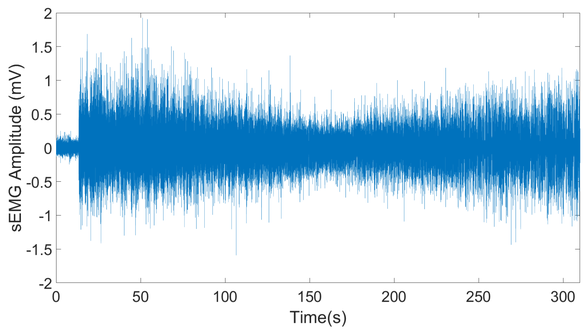

Figure 1: Raw EMG signal over a 5-minute trial period. The data is very noisy and difficult to see trends in.

Goal: Develop a streamlined method of classifying muscle fatigue to help with stroke rehabilitation and treatment of neuromuscular conditions.

Methods

Subjects: 17 neurologically intact females and 14 neurologically intact males between ages of 18 and 32

Data Collection:

- Delsys mini sEMG sensor placed on subject (Figure 2)
- Subjects maintained 50% of max voluntary contraction for 5 minutes (Figure 3)

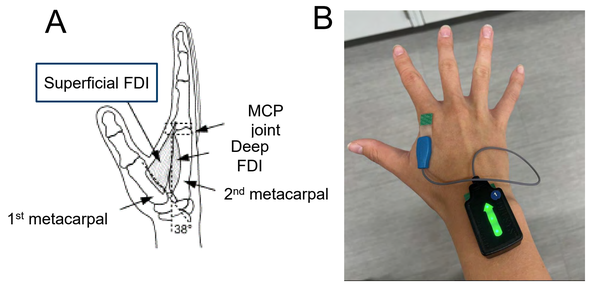

Figure 2: A) Location of superficial first dorsal interossei (FDI) muscle (blue box). Adapted from [3]. B) Placement of sEMG electrode on the FDI muscle with ground electrode on wrist

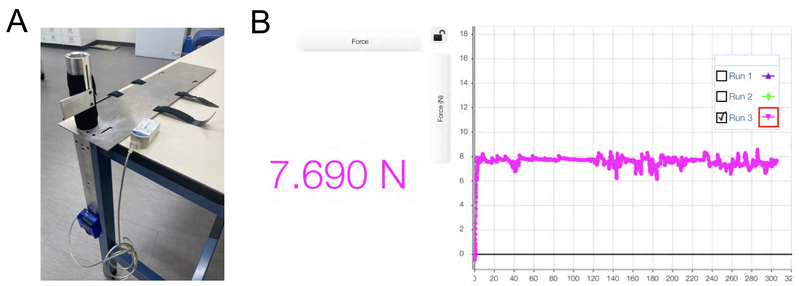

Figure 3: A) Experimental setup to stabilize and isolate FDI muscle. B) Live force feedback provided during data collection for the subject

- *Traditional analysis:* Filtered raw data, segmented into 20 second intervals, and converted to the frequency domain by Fast Fourier transform (FFT) (Figure 4)
- *Machine learning*: Raw sEMG signal reconstructed in the phase space for topological data analysis

Results

- Mean and median frequency (MNF and MDF) decreased between intervals (Figure 4)

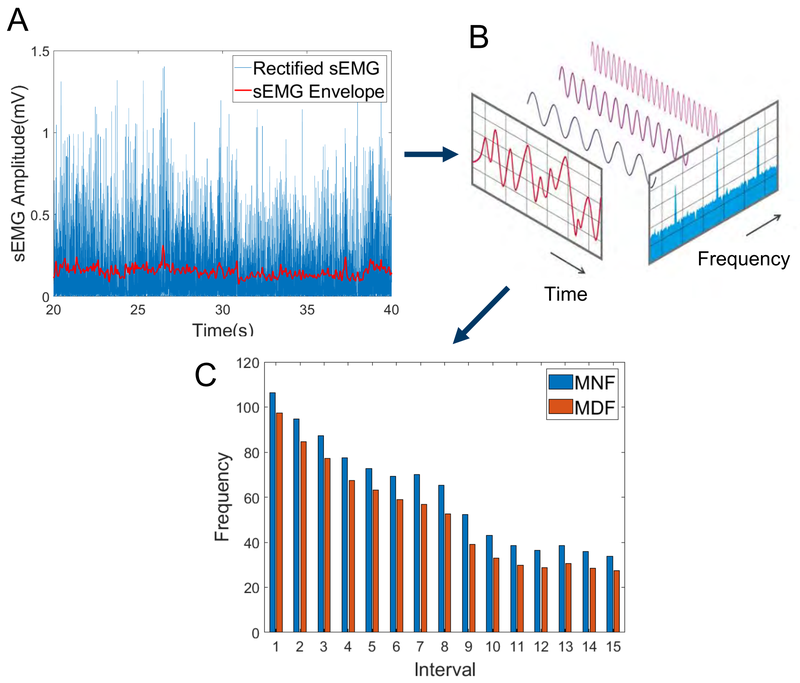

Figure 4: A) Rectified sEMG data and envelope of 20 second interval. B) Schematic of FFT [4]. C) MNF and MDF over 20 second time intervals.

- Preliminary visual analysis of phase space point clouds show topological differences between fatigued and non fatigued sEMG data (Figure 5)

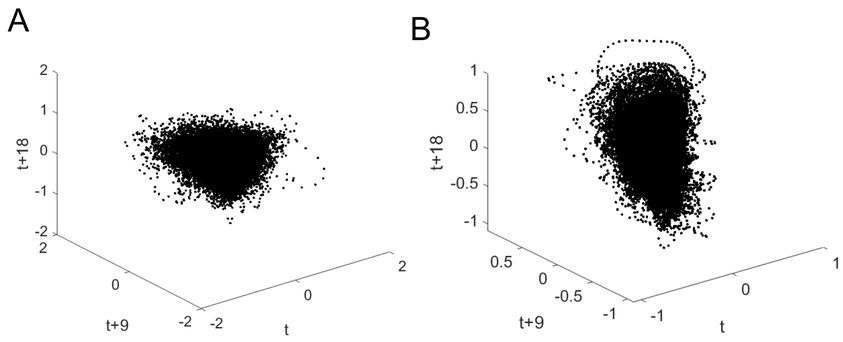

Figure 5: Phase space reconstruction of the sEMG signal from 20-40 seconds (A) and 200-220 seconds (B)

Conclusions and Future Work

- Traditional analysis clearly shows fatigue of the FDI
- Continue the machine learning procedure:
  1. Phase space → persistence barcode
  2. Fit kernel regression to persistence barcode
  3. Train algorithm on labeled data, then test with new data
- Integrate relationship of force, frequency, and fatigue
- Comparison between traditional analysis classification and machine learning algorithm classification

Acknowledgements

The authors would like to thank the Program for Undergraduate Research (PUR) at Bucknell University for funding this study.

References

[1] Zhou, Ping, et al. *J. Neural Eng.* 2011. doi: 10.1088/1741-2560/8/3/036028
[2] Phinyomark, Angkoon, et al. *Computational Intelligence in Electromyography Analysis.* 2012. doi: 10.5772/50639
[3] Hudson, Anna L., et al. *J. Physiol.* 2009. doi: 10.1113/jphysiol.2008.165043
[4] "Fast Fourier Transformation FFT- Basics" *NTI Audio*

What is the fastest way to process your data while keeping it secure?

Tyler Hargus & Dr. David Chang

Susquehanna University

INTRODUCTION

- ChaCha20-Poly1305 and AES-GCM are cryptographic algorithms that are used to secure and authenticate vital data or information transmitted over a network
- ChaCha20-Poly1305, which is a AEAD (Authenticated Encryption with Additional Data), is mainly used to secure and protect internet security over the web using SSH (Secure Socket Shell) or through TLS (Transport Layer Security)
- AES-GCM (Advanced Encryption Standard-Galois Counter Mode) is used to provide high security to sensitive information by protecting and authenticating data on electronics and or computers
    - In fact, AES is used by the National Security Agency to protect the sensitive data within the Agency
- Encryption is vital to protecting one's data from hackers or unauthorized personnel trying to intercept transmitted or stored personal data on one's system
- These algorithms are used daily whether it be through messaging platforms over a network or storing data on your device
- We are testing and implementing these algorithms into an Echo Server based platform to send and receive messages over a networked environment while providing cryptographic algorithms to provide security and authentication
- We are analyzing both algorithms to test which platform performs the fastest over a Bare-PC (OS-less) system

OBJECTIVES

- Test the processing time of encryption and decryption for ChaCha20-Poly1305 and AES-GCM algorithms on a Bare-PC system while developing software on Windows and Linux systems
- Testing, with pending results, that the cost of processing time of a Bare-PC is faster for incoming versus outgoing packets for AES-GCM and ChaCha20-Poly1305 over a networked environment
- Proving that a Bare-PC system performs faster than a Windows or Linux system with these algorithms applied and transmitted over a network

METHODS & PROCEDURES

- Obtain Bare-PCs, Cat6E Ethernet Cable, network switch, Windows, and Linux systems to develop software on
- Develop Echo Server software in C programming language to send and receive messages through a server and client
    - Developed software on Linux and Windows OSs
    - Create a TCP (Transmission Control Protocol) and UDP (User Datagram Protocol) versions for both Windows and Linux to perform over a networked environment
- Apply ChaCha20-Poly1305 and AES-GCM algorithms to the developed versions of the Echo Server software to provide the encryption and decryption functionality

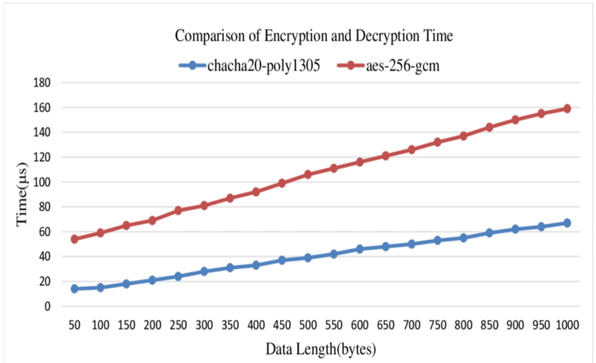

Figure 1 displays that ChaCha20-Poly1305 is substantially higher in performance compared to AES-GCM. ChaCha20-Poly1305 has a faster speed and reduces power consumption on the hardware used[1]

- Test the functionality of the software over Windows and Linux OSs to confirm that the program runs properly
- Apply the developed software to the Bare-PC system over the networked environment
- Set and open a server over the networked environment to have the clients connect and send messages
    - Have the client send plain text strings to and from the server and client over the network
- Once the server receives messages, test the speed varying on the algorithms used to calculate which encryption and decryption method works the quickest while providing the proper security and authenticity to the messages

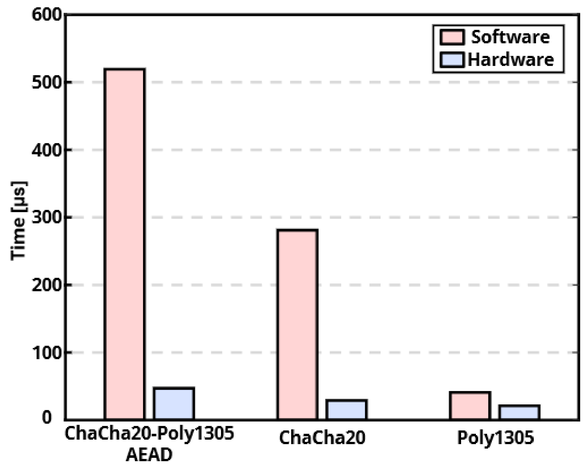

Figure 2 shows the comparison between software and hardware implementations with the AEAD. The AEAD increased by 968%, 195%, and 1104% compared to the other software implementations[2]

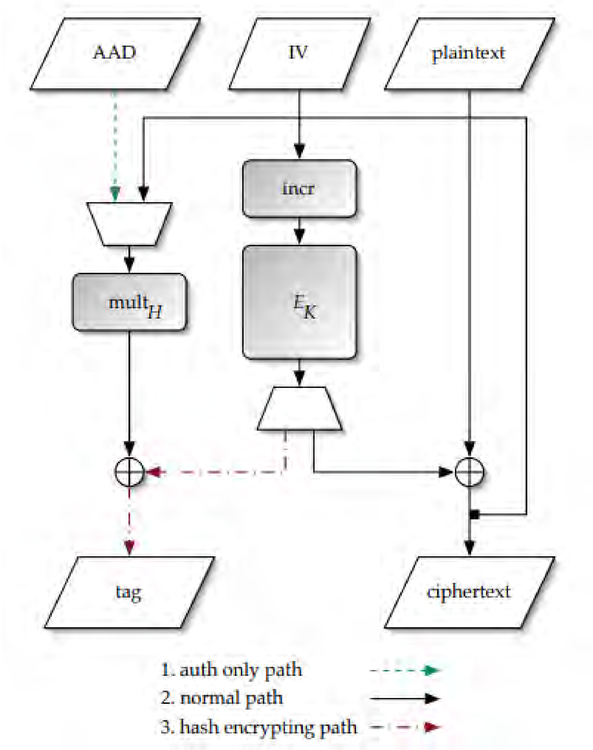

Figure 3 shows the hardware implementation of GCM and describes the various paths through a circuit this algorithm takes[3]

ESTIMATED CONCLUSIONS & RESULTS

- We introduced the implementation of the ChaCha20 and Poly1305 hardware primitives in addition to a compatible ChaCha20–Poly1305 AEAD construction with an Echo Server on Linux, Windows, and Bare-PC systems
- The proposed AEAD implementation was tested on a Bare-PC by comparing Linux and Windows OSs
    - In addition, the function of the length of the plaintext and the AAD are supported
- The Bare-PC system shows an increase of performance by 30.76% in the Linux and Windows systems implemented with a 40.64% area overhead, using the same transactions in the previous work
- In comparison with the related works, the performance of the AEAD is 1.4 and 11.56-cycles/byte in standalone and system implementations, increasing the performance by 1517% in the standalone implementation
- Finally, the ChaCha20–Poly1305 implementation is compared with another AEAD used in an Echo Server on a Bare-PC system, demonstrating the competitive performance resources with the AES-based cipher suites

ACKNOWLEDGEMENTS

- Susquehanna University
- Dean Kathy Straub
- Dr. Karne and Alexander Wijesinha from Towson Universitys

REFERENCES

1. Kao, T L, et al. "Performance of AES-GCM and Chacha20-Poly1305 on Zedboard." *Researchgate.net*, Sept. 21AD, https://www.researchgate.net/figure/Performance-of-AES-GCM-and-ChaCha20-Poly1305-on-Zedboard_fig1_354738575
2. Serrano, Ronaldo, et al. "Chacha20–Poly1305 Authenticated Encryption with Additional Data for Transport Layer Security 1.3." *MDPI*, Multidisciplinary Digital Publishing Institute, 17 June 2022, https://www.mdpi.com/2410-387X/6/2/30/htm
3. McCrew, D. A., & Viega, J. (n.d.). *The Galois/counter mode of operation (GCM) - unibs.it*. luca-giuzzi.unibs.it. Retrieved July 20, 2022, from https://luca-giuzzi.unibs.it/corsi/Support/papers-cryptography/gcm-spec.pdf s

Susquehanna UNIVERSITY

ProPANE Notetaking Assistive Technology

Bangyan Li & Quan Nguyen Tu

Department of Education and Electrical & Computer Engineering

Advisors: Janet VanLone, M. Stu Thompson, Robert M. Nickel

Bucknell University, Lewisburg, PA

Project Overview

What is ProPANE?

The ProPANE notetaking assistive technology is a collaborative project between Electrical & Computer Engineering and Education at Bucknell University.

What is the overarching project goal?

To develop an assistive technology that will support notetaking for college students with certain learning disabilities (LD) and English Language Learners (ELLs) in the lecture-based classroom to improve their content learning and academic performance.

We intend to do:

- reduce students' cognitive load and free students' working memory space to absorb lecture content
- extract information from the lecture for the student to further review and/or annotate
- allow the student to focus more on the lecture and not note taking in order to engage in other ways and use their working memory space on activities and discussion.

What is the rationale?

In higher education, course instructors most often utilize lectures to deliver content information to students. While support for developing effective note-taking strategies is often provided to all students in high school, college students are typically expected to already have good note-taking skills. Students with LDs and ELLs often face challenges with taking notes in college classrooms, however, they must learn high-level thinking, problem-solving skills, and comprehend difficult content while simultaneously using listening, processing, note-taking, and organizational skills (Williams & Eggert, 2002[1]).

Explicit Instruction Diagram

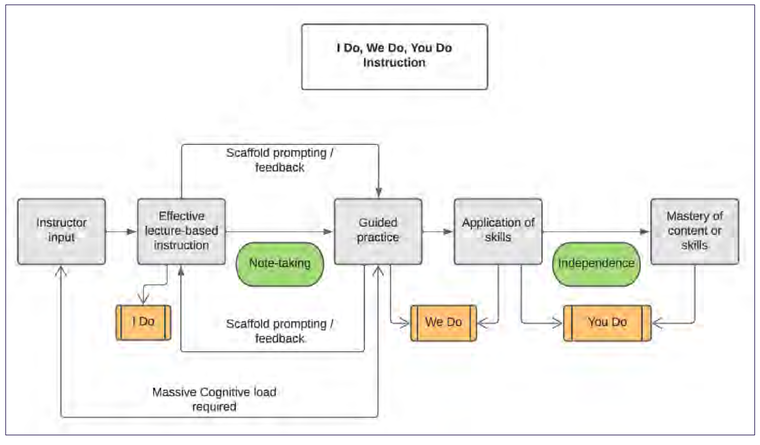

Education

Research Studies		
	Study 1 (Staff; n=89)	Study 2 (Students; n=39)
Primary Research Questions	• What notetaking supports are available to students in your institution? • What are the biggest note-taking challenges for students?	• What challenges do you face while taking notes in a lecture-based classroom? • What strategies do you use to take good notes?
Methods	Quantitative methodology: Survey including open and closed ended questions	Quantitative methodology: Survey including open and closed ended questions
Results*	• 46 responses agreed the biggest challenges for students to take effective notes is that students do not know what's the most important point of the lecture-based courses • 48 responses allowing students to use laptops as accommodation to help students to take notes	• 20 students regarded lecture pace is too fast and distinguish important contents which challenges them to take effective notes • 22 students expressed that they have not used assistive technology to take notes
Next Steps	• Analyze survey data	• Analyze survey data • Conduct semi-structured interviews

**Preliminary results as of July 2022*

**130 PA institutions invited to participate in this project*

Technology

We have made some initial attempts using traditional image processing techniques and found out those are insufficient. As such, we are now utilizing supervised machine learning using labeled data generated by a 3D camera, which utilizes a laser to record distance for each pixel. The distance measure between the camera and the board as well as the distance between camera and obstruction will be different, which allows us to distinguish between what is the board and what is the obstruction. The obstruction identification results from the videos with the 3D information will then be used to train a machine learning algorithm to identify obstruction information from regular 2D videos.

Color image

Depth information

Labeled data

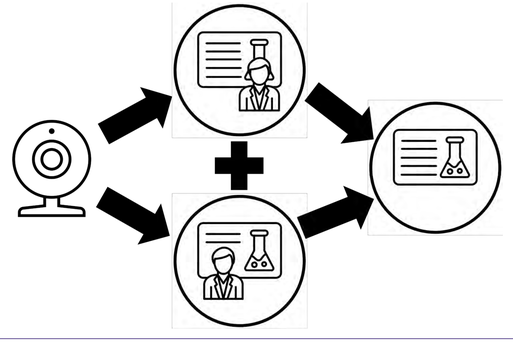

The algorithm will then eliminate the obstruction by combining different frames of the videos, creating an unobstructed view of the board. This will output the content of the board as a section in an electronic report that summarizes the entire lecture.

Challenges

- ❑ Get diverse population
- ❑ Processing incorrect data:

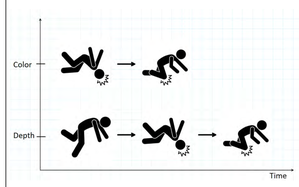

Time drifting when the obstruction is in motion, resulting in "phantom effect"

Non-reflective surface (such as hair) may not provide depth information, as the laser doesn't bounce back

Future Developments

- ❑Gather survey data to conduct semi-structured interviews
- ❑Analysis survey and interview data to advance features of the notetaking assistive technology
- ❑Develop a focus group to test mock application and update the notetaking assistive technology
- ❑Develop a supervised machine learning model using labeled data to optimize and automate the process.
- ❑Create a smartphone application and a server that could record videos and send them to a back-end system for processing.

References

[1] Williams, R. L., & Eggert, A. C. (2002). Notetaking in college classes: Student patterns and instructional strategies. The Journal of General Education, 173-199.

Acknowledgements

We would like to thank the following sponsorships for making this project possible.

- ❑ Ciffolillo Healthcare Technology Inventors Program (HTIP)
- ❑ Sojka Research, Teaching, and Scholarships in Developmental Disabilities, Neuroscience & Human Health Annual Fund
- ❑ Bucknell Program of Undergraduate Research

Analysis of Upper Extremity Joint Kinematics and Surface Electromyography

Sarah H. Vestal[1], Benjamin B. Wheatley[1], Chulhyun Ahn[2]

[1]*Department of Mechanical Engineering, Bucknell University, Lewisburg PA*
[2]*Department of Physical Medicine and Rehabilitation, Geisinger, Danville PA*

Mechanics and Modeling of Orthopaedic Tissues Lab

Introduction

- Every year, more than 795,000 people in the United States have a stroke [1]
- The human central nervous system (CNS) adopts a modular control strategy, rather than controlling muscles individually-muscle synergies [2]
- Muscle Synergy based rehabilitation has had success in restoring impaired motor modules, but is costly and unavailable

Goal: Identify individual kinematic synergies that are linked to individual electromyography (EMG) synergies in healthy adults.

Methods

- Subjects perform set of predefined upper extremity (UE) movements to mimic daily activities
- Joint angles determined through an inverse kinematics analysis (Figure 2)
- Process and normalize EMG data to maximum voluntary contractions (MVC) (Figure 3)

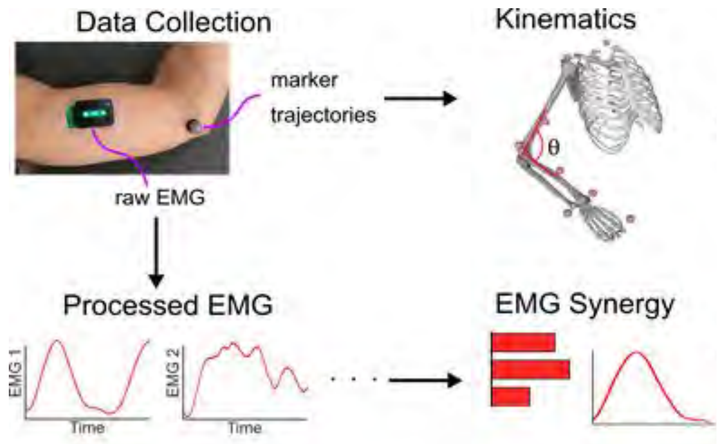

Figure 1. Marker trajectories and surface EMG are collected in the lab. Once the data is processed synergies can be extracted.

Results and Discussion

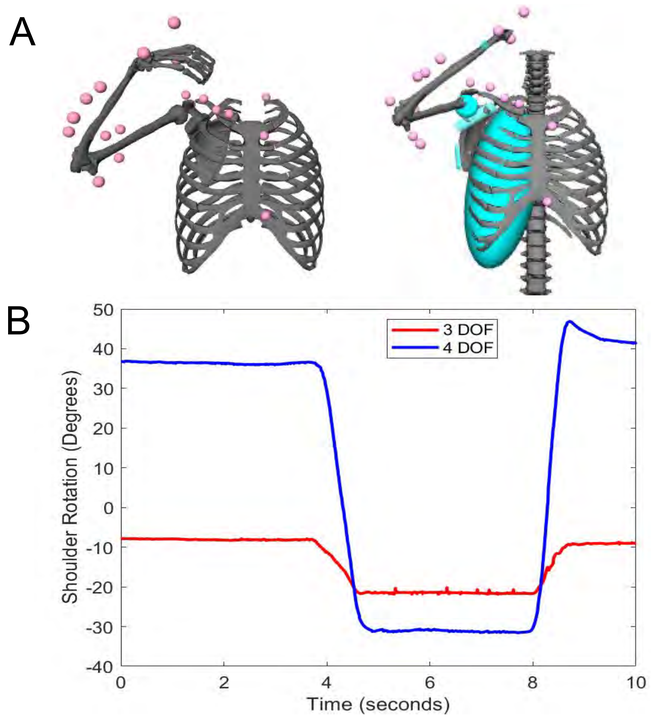

Figure 2. A) UE models with three degrees of freedom (left) versus four degrees of freedom (right) and B) their corresponding axial rotation in degrees during the zipper movement.

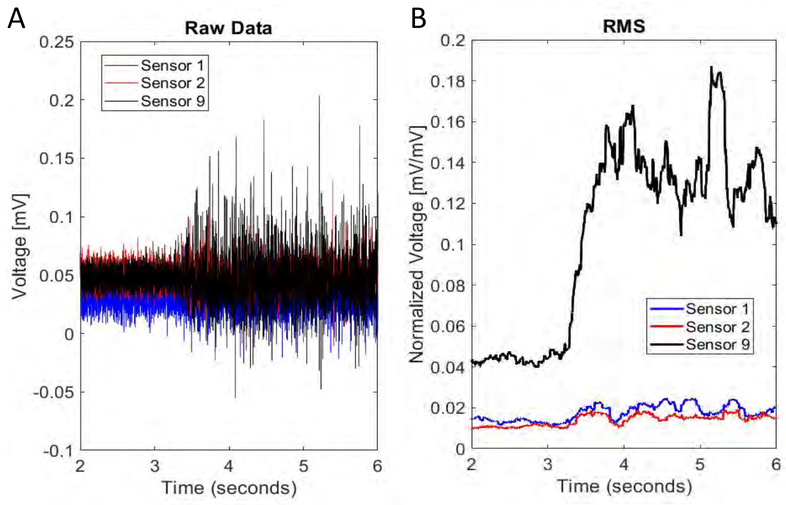

Figure 3. A) Raw sEMG data from zipper activity. B) Normalized root square mean (RMS) values for the same sensors and activity.

Future Work

- Complete data collection from 20 healthy adults
- Subjects will later be asked to generate an UE movement that produces the same surface EMG profile as the EMG synergies with visual feedback
- Distinct arm kinematics derived from the EMG synergy will be labeled as the kinematic synergy

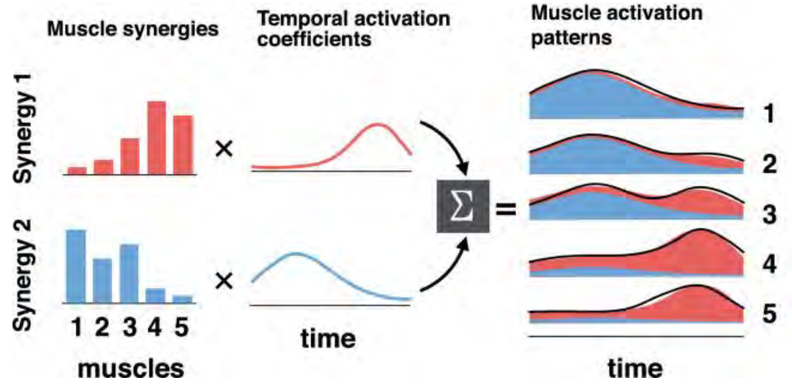

Figure 4. Representation of muscle activations and their reconstruction by the synergy model. [4]

Acknowledgements

The author would like to thank the emerging scholars program at Bucknell University for funding this summer research.

References

[1] Tsao, C., et al. *Circulation.* 2022. doi: 10.1161/CIR.0000000000001052
[2] Ting, L., et al. *Neuron.* 2015. doi: 10.1016/j.neuron.2015.02.042
[3] Seth A., et al. Front Neurorobot. 2019. doi: 10.3389/fnbot.2019.00090/full
[4] Yokoyama, H., et al. Sci Rep. 2021. doi: 10.1038/s41598-021-98022-8

The histone H2A variant H2A.Z regulates the expression of TOR signal genes in the yeast *Saccharomyces cerevisiae*

Brianna Watts, Olivia Geesaman, Emma Oley, and Dr. Michael Parra
Department of Chemistry, Susquehanna University, Selinsgrove, PA

Abstract

Nucleosomes are comprised of two copies of each of the canonical histones: H2A, H2B, H3, and H4. In Saccharomyces cerevisiae H2A.Z, an H2A variant, replaces canonical histone H2A in about 10% of nucleosomes. Histone H2A.Z has distinct functions from histone H2A and is involved in transcriptional regulation, DNA damage response, and heterochromatin silencing. Rapamycin (sirolimus) is an antifungal drug that inhibits protein synthesis and arrests the cell cycle. GTP binding protein Resemblance (GTR1) is upregulated in the presence of rapamycin and activates the target of rapamycin complex 1 (TORC1) in response to amino acid stimulation. H2A.Z deletion leads to repression of *GTR1* in the presence of rapamycin which is the likely reason for intermediate rapamycin sensitivity in the htz1Δ strain. We hypothesize that a htz1Δ/gtr1Δ strain will exhibit extreme sensitivity to rapamycin and we can rescue this sensitivity by overexpressing *GTR1*. This will demonstrate a direct genetic interaction between *GTR1* and *HTZ1*.

Figure 1: The nucleosome core particle

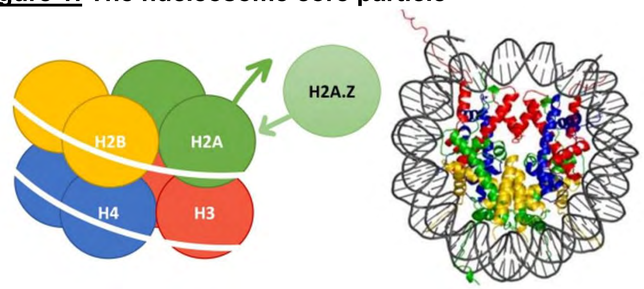

Figure 1: The nucleosome core particle (NCP) is composed of two of each of the canonical histones: H2A, H2B, H3, and H4. H2A.Z is a functional and structural homolog with 65% identity that replaces H2A in about 10% of nucleosomes. Loss of H2A.Z is tolerated in *S. cerevisiae*.

Table 1: Yeast strains

Strain Name	Genotype	Purpose
BY4741	MATa; his3Δ1; leu2Δ0; met15Δ0; ura3Δ0	Wild-type control
YMP050	MATa; his3Δ1; leu2Δ0; met15Δ0; ura3Δ0; htz1::KanMx	htz1Δ in BY4741 background
YMP334	MATa; his3Δ1; leu2Δ0; met15Δ0;ura3Δ0; gtr1::KanMx	gtr1Δ for rapamycin study

Table 1. Genotypes and purposes of yeast strains used in this study.

References

1. Geesaman, Olivia, Oley, Emma, Galliher, Kaitlyn, Nattress, Taylor, Harling, Emily, Winters, Nickolas, Blatt, Isaiah, Watts, Brianna, and Parra, Michael A. "The histone H2A variant H2A.Z regulates the expression of TOR signal genes in the yeast *Saccharomyces cerevisiae*" in preparation
2. Brachmann, Carrie Baker, Davies, Adrian, Cost, Gregory J., Caputo, Emerita, Li, Joachim, Hieter, Phillip, Boeke, and Jeff D. (1998) Yeast "Designer Deletion Strains derived from *Saccharomyces cerevisiae* S288C: a Useful set of Strains and Plasmids for PCR-mediated Gene Disruption and Other Applications"

Figure 2: Loss of H2A.Z leads to rapamycin sensitivity in yeast

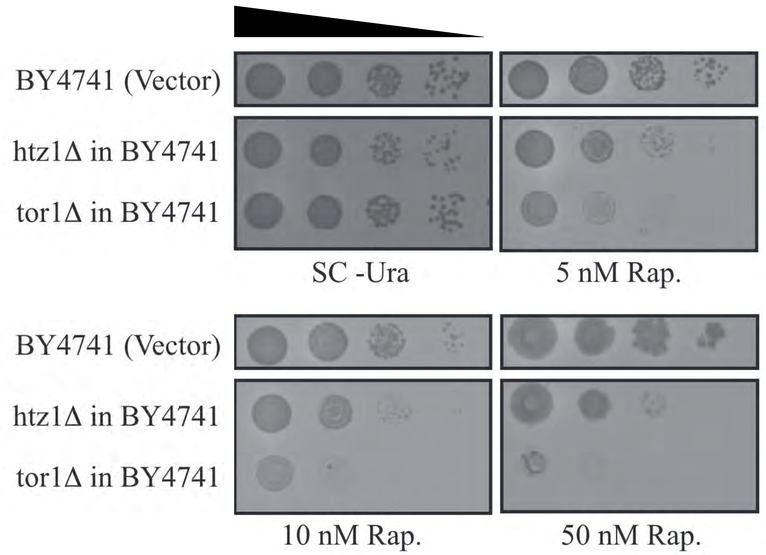

Figure 2: Strains bearing the indicated gene deletions were grown overnight in synthetic complete without uracil (SC-Ura). Strains were diluted to a final OD_{600} = 0.5, serially diluted 10-fold in sterile water, and spotted onto media containing rapamycin at the indicated concentrations. Plates were incubated for 2-4 days at 30°C. Wild-type and htz1Δ strains in the BY4741 background. A tor1Δ strain was used as a control.

Figure 3: *GTR1* mRNA levels are lower in htz1Δ relative to wild-type

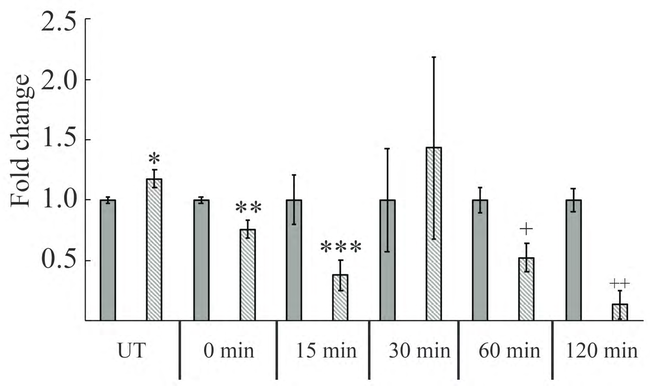

Figure 3: *GTR1* mRNA levels are lower in htz1Δ relative to wild-type in the presence of rapamycin over the course of 120 minutes. The solid gray bars represent wild-type data while the bars with the diagonal gray lines represent the htz1Δ data. The average and standard deviation of a minimum of at least three or more independent experiments for each mutant are plotted and statistical significance determined by t-test. **P < 0.15; **P < 0.1; ***P < 0.015; + P<0.2; ++ P<0.09*

Acknowledgements

We would like to thank Susquehanna University, the S-STEM program (NSF grant #1742506), and the McGrath Scholars Program for financial support for this project. We would also like to thank Dr. Brian Strahl for the yeast strains used in this study. I would also like to thank my fellow lab members for their contributions to this study.

Figure 4: PCR-mediated gene disruption of *GTR1* in BY4741 and htz1Δ

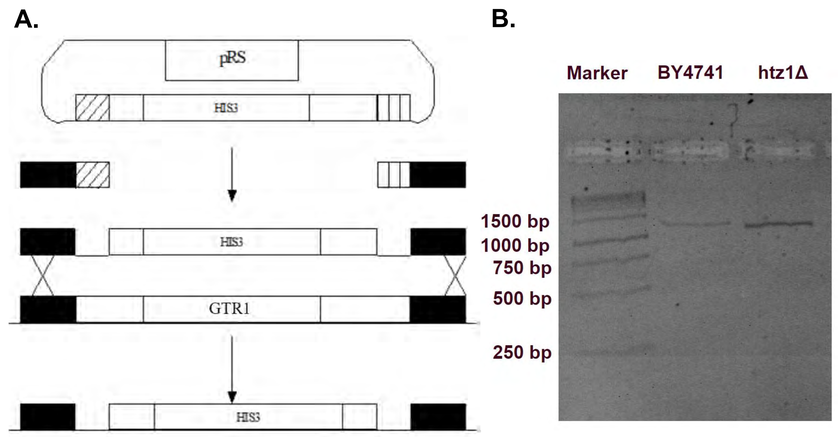

Figure 4: A. The schematic indicates the process by which *GTR1* will be replaced by *HIS3* in BY4741 and in htz1Δ strain. Positive transformation will yield two new strains of yeast, gtr1Δ and htz1Δ/gtr1Δ. It is hypothesized that deletion of both *HTZ1* and *GTR1* will confer a greater sensitivity to rapamycin. This sensitivity can be rescued by over-expressing *GTR1*. **B.** The PCR gel image indicates how positive transformation is determined. The first well contains the molecular weight marker, which allows the size of the amplicon to be determined. The second well contains BY4741(control) and the third well contains htz1Δ. *HIS3* is larger than *GTR1*, at 1384 bp and 1132 bp, respectively. Since the two amplicons in the image are the same size, it indicates that the transformation was not successful.

Figure 5: The plasmid used for the overexpression of *GTR1*

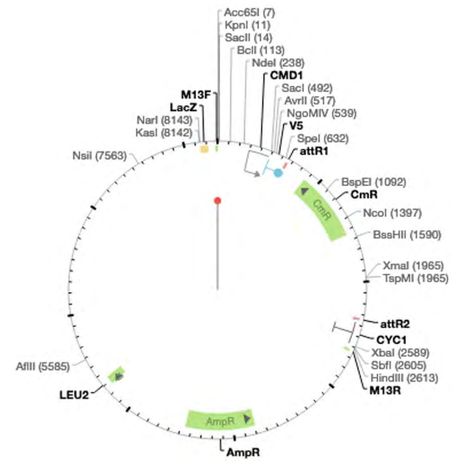

Figure 5: Yeast/*E. coli* shuttle vector plasmid used for the overexpression of *GTR1* in htz1Δ and htz1Δ/gtr1Δ strains. The plasmids are isolated from *E. coli* before undergoing purification and transformation into yeast. *GTR1* can be overexpressed due to the inducible promotor located 5' of the gene. Overexpression of *GTR1* will rescue rapamycin sensitivity and indicate a direct genetic interaction between *GTR1* and *HTZ1*.

Conclusions

- Deletion of *HTZ1* confers intermediate rapamycin sensitivity
- *GTR1* is upregulated in the presence of rapamycin
- In the presence of rapamycin, *GTR1* mRNA levels are lower in the htz1Δ strain than the wild-type
- *HTZ1* likely regulates *GTR1*

Synthesis and Optical and Electrochemical Properties of Squaraine-Based Dyes

Eric Ressler, Nicole Kahler, Emily Carr, Phillip Brogdon
Department of Chemistry, Susquehanna University, Selinsgrove PA 17870

Abstract

Squaraine-based dyes are strongly absorbing, often highly fluorescent materials that can readily be prepared in a single step from squaric acid and a nucleophilic species. Various activated aromatic reactants can be created and modified to tune the optical and electronic properties of the final dyes. Due to their ability to absorb and emit light in the visible region of the electromagnetic spectrum, squaraine dyes find application as photosensitizers in photovoltaic devices and as emissive materials for applications such as biological imaging and chemosensors. In this work, indole- and aniline-based donors were used in a condensation reaction with squaric acid to produce the target dyes. In addition to their synthesis, dye properties were also analyzed using UV-vis absorption spectroscopy, emission spectroscopy, and cyclic voltammetry to study the effects of the differing electron donors on the dye design.

Background

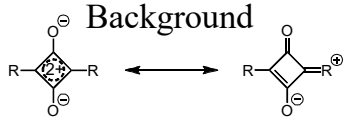

Figure 1: Resonance structures of squaraine dyes.

- General structure of a squaraine dye uses squaraine as an electron acceptor, with two electron donating groups lending to the core
- In the second resonance structure, the squaraine core acts as a bridge as one R group donates and the other accepts
- When light is absorbed, the conjugated structure allows the excited electron to travel throughout the molecule, resulting in strong absorbance and emission

Target Molecules

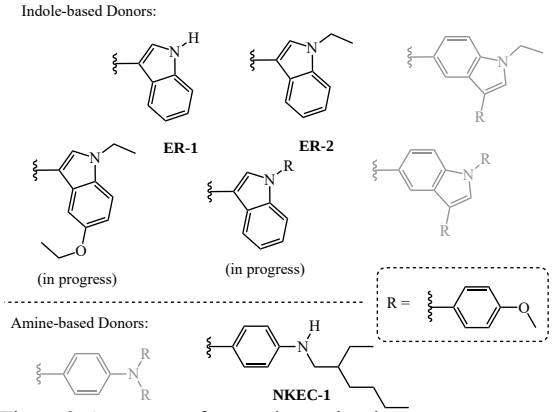

Figure 2: Structures of target dye molecules.

Synthesis

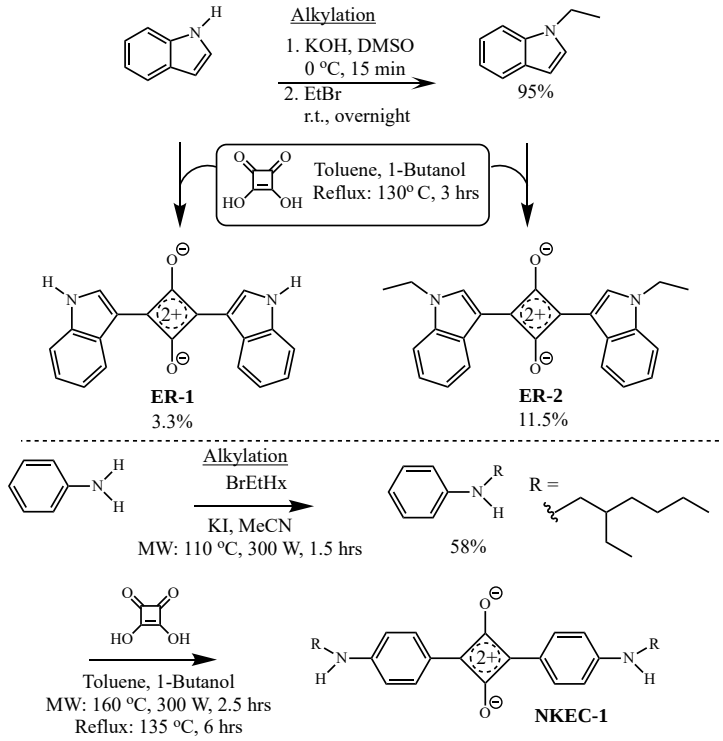

Figure 3: Synthesis of squaraine dyes with varying donors and alkyl chains.

Electrochemical Data

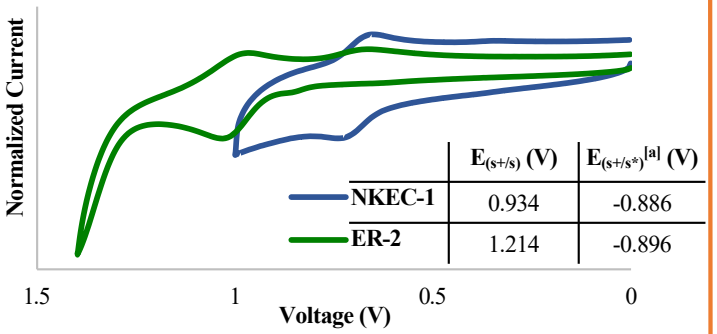

	$E_{(s+/s)}$ (V)	$E_{(s+/s^*)}$[a] (V)
NKEC-1	0.934	-0.886
ER-2	1.214	-0.896

Figure 4: Raw cyclic voltammetry data for **NKEC-1** and **ER-2**, with current normalized to **ER-2** in DCM. CV values were calibrated with ferrocene as an internal standard (0.7 V vs NHE). [a]$E_{(s+/s^*)}$ is $E_{(s+/s)} + E_g^{opt}$ from the optical data to find the energy of the excited state.

Optical Data

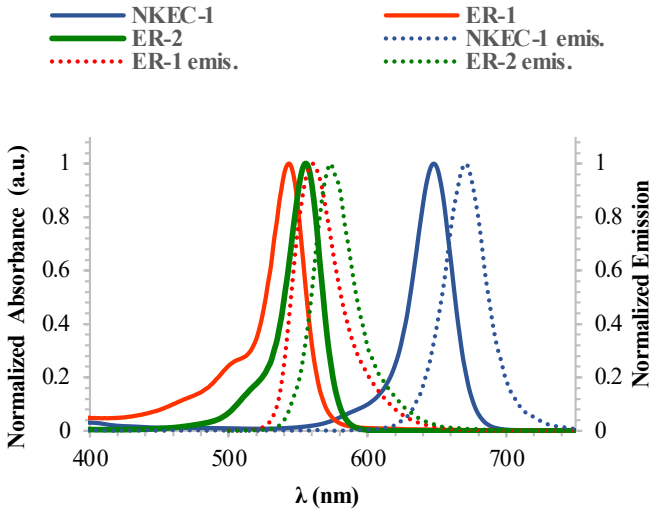

Figure 5: UV-vis absorbance and emission curves of synthesized dyes in acetone.

Table 1: Absorbance and emission data for synthesized dyes in acetone. [a] λ_{max} was determined at the peak of the lowest energy transition. [b] Optical band gap (E_g^{opt}) was calculated using $E = (hc / \lambda_{onset})$.

Dye	λ_{max} (nm)[a]	λ_{onset} (nm)	λ_{emit} (nm)	E_g^{opt} (eV)[b]
NKEC-1	648	680	671	1.82
ER-1	543	573	561	2.17
ER-2	556	589	573	2.11

Future Work

- Determine the molar absorptivity of the synthesized dyes
- Explore the pH dependance of the UV-vis absorbance spectra as observed in **ER-1**
- Determine excited state lifetimes and emission quantum yields
- Perform computational studies to determine optimized structure and orbital distributions

Acknowledgements

Funding for this research was provided by Susquehanna University and the Summer Research Partners program.

Incidental Discovery of a Left Ventricular Mass in an Octogenarian with Metastatic Squamous Cell Lung Cancer

By: Christopher D. Manko, Steven J. Grampp, and Stephen Voyce
Geisinger Commonwealth School of Medicine

Introduction

- Cardiac Fibromas are a rare type of tumor that grow in the myocardium
- They typically are found in children

Case Report

- An 83-year-old patient presents with squamous cell lung carcinoma
- Upon imaging, a heart mass was located and determined to be a cardiac fibroma
- Given his past medical history, surgical intervention did not occur

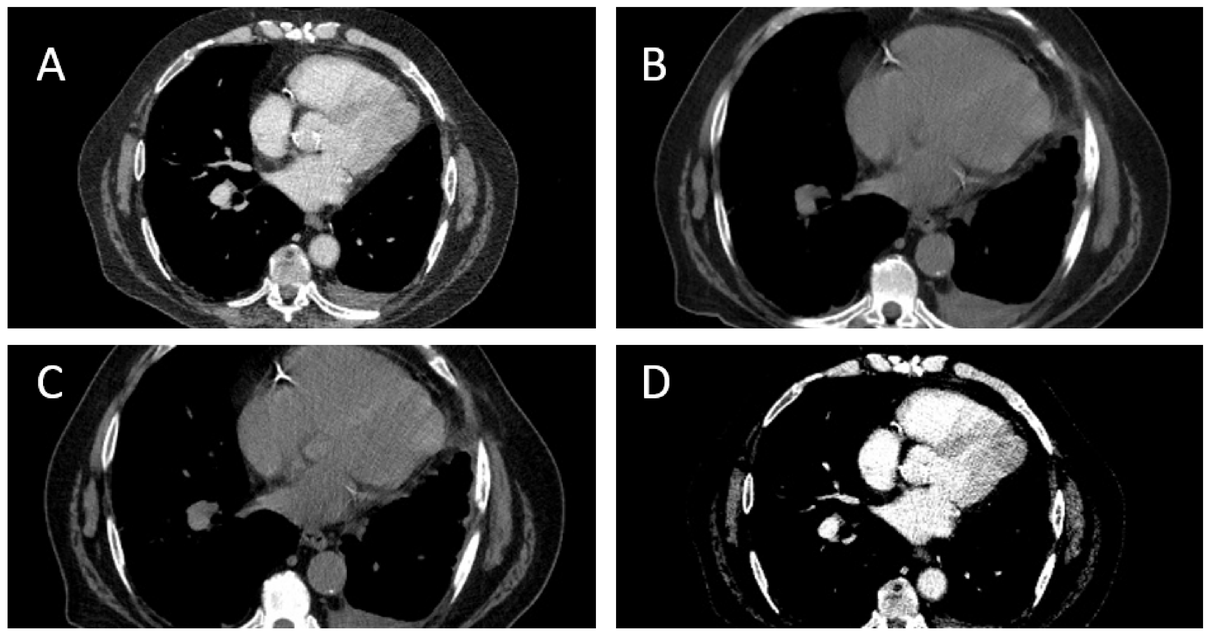

Figure 1 illustrates multiple CT images of the cardiac fibroma

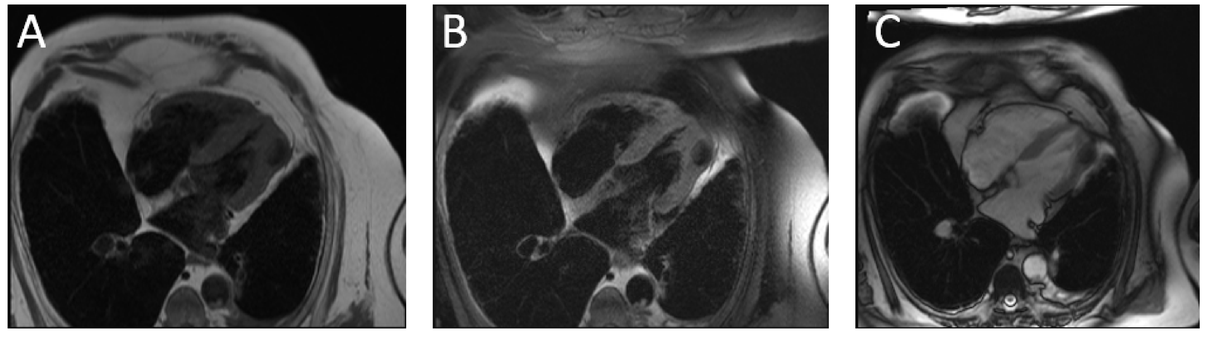

Figure 2 depicts 3 MRI images taken of the tumor

Discussion

- In adults, secondary tumors are far more common than primary
- Clinical symptoms can vary greatly
- No standard treatment plan currently, but surgical and pharmacological interventions available

Conclusion

- This case presents a patient with a very rare cardiac fibroma not commonly found in his respective age group
- Imaging is a vital component of medical investigation to reach a proper diagnosis

Meiotic Segregation of the Sex Trivalent System in *Hierodula membranacea*

Riley E. Beebe, Morgan L. Thomas, Zhengkai Zhu, Dr. Leocadia Paliulis.

Department of Biology, Bucknell University, Lewisburg, Pennsylvania

Abstract

Meiosis, the creation of haploid gametes from a diploid parent cell, is essential for producing the genetic variability that distinguishes sexual reproduction. In the traditional meiotic program, bivalent homologous chromosomes pair and segregate via regulated and balanced microtubule tension forces. However, exceptions to this program occur, notably within the model organism, *Hierodula membranacea,* which contains a trivalent sex system. The trivalent arrangement proposes a unique modification within meiosis where sex chromosomes are unequally paired, yet progress throughout the meiotic program without abnormalities. Here we will explore the trivalent system to study chromosome position and interactions which regulate its segregation. Through live cell and confocal imaging, microtubule tension forces and meiotic behavior can be further elucidated. Our study anticipates that the Y chromosome microtubule tension forces are equally as strong as those of X_1 and X_2 combined.[3] The trivalent arrangement in *Hierodula membranacea* cells will develop current understandings of the biophysical mechanisms associated with human congenital ailments, and further reveal how balanced tension forces work to properly segregate chromosomes.

Introduction

- Meiosis I is the first program of cellular division and is the stage where sex chromosomes segregate and ploidy decreases in half (Figure 1).
- The trivalent structure and behavior is only visualized throughout Meiosis I.
- Correct chromosome alignment and subsequent segregation during anaphase are important to successful cellular division. In order to segregate, the microtubules have to apply a specific amount of tension to the kinetochores of each chromosome on the metaphase plate. [2]
- Microtubule tension is balanced evenly in a bivalent sex system, such as one containing XX and XY. In a trivalent sex system, such as in *Hierodula membranacea* where three sex chromosomes connect and align for segregation, the tension forces are also balanced (Figure 5).
- Knowledge about how this trivalent system maintains microtubule balance is not fully revealed and may be useful for understanding how congenital disorders such as trisomy 21 occur during cell division.
- To understand the behavior of the trivalent sex system, spermatocytes of male *H. membranacea* are imaged using live cell microscopy, immunofluorescent staining, and confocal microscopy.

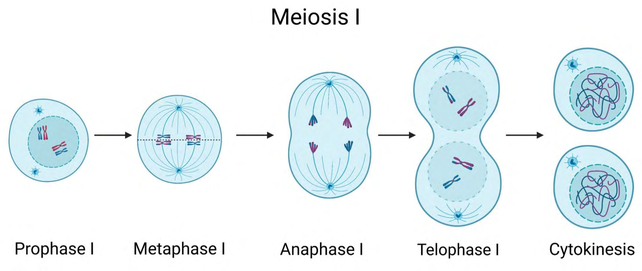

Figure 1. Meiosis I program

Methods

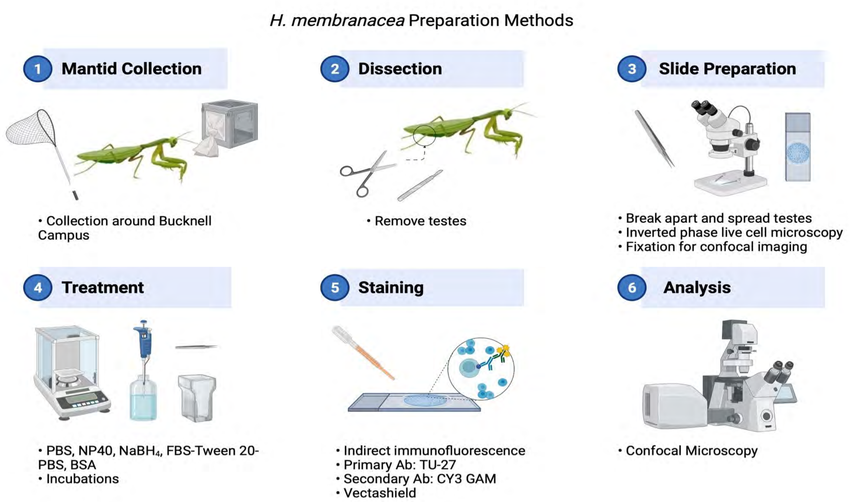

Figure 2. Dissection and slide preparation methods for live cell imaging and confocal microscopy analysis

Results

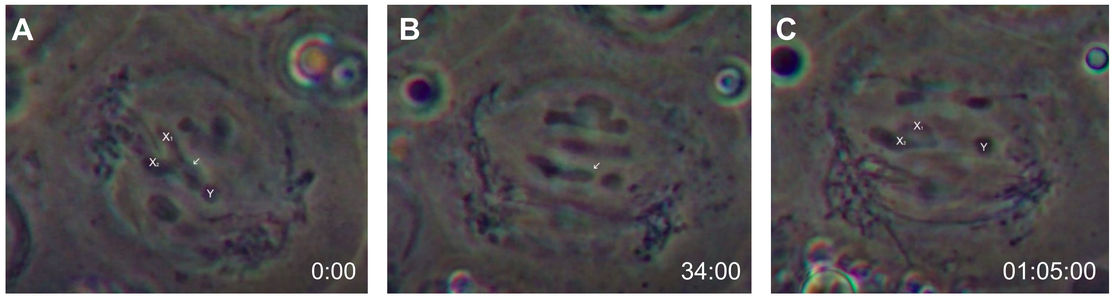

Figure 3. Metaphase I through late anaphase I of an *H. membranacea* spermatocyte using live cell imaging via inverted phase microscopy. The tivalent system (marked by white characters and an arrow) aligns on the metaphase plate (A, 0 min). At early anaphase I onset, the trivalent system initiates segregation (B, 34 min). In late anaphase I, the trivalent elongates and separates from homologues (C, 65 min).

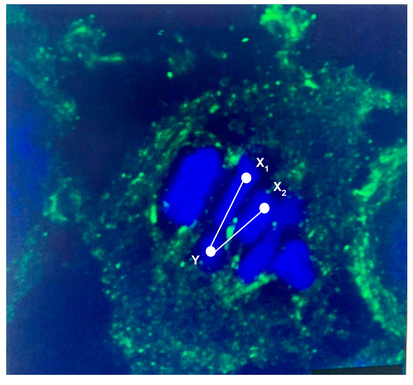

Figure 4. Confocal image of spermatocyte cell in metaphase. DAPI blue immunofluorescence staining of genetic material and Cy3 green immunofluorescence of of microtubules. Poor microtubule preservation leads to reduced visibility of microtubule bundles.

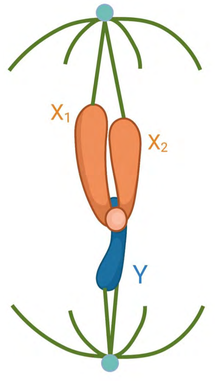

Figure 5. Graphic render of the trivalent system.

Discussion

Results from preliminary confocal microscopy indicate poor microtubule visualization, a result from the quality of cell fixation, that ultimately obstructed the collection of desired trivalent images. Slides were initially prepared using chromosome spreads. This technique failed to yield quality spermatocyte cells for visualization (Figure 4). This challenge was addressed by performing chromosome squashes that utilized liquid nitrogen. While confocal images have improved, further challenges to troubleshoot remain, and areas of optimization include:

- Cell fixation during metaphase and anaphase stages
- Dissection of mantid testes before maturity
- Microtubule preservation
- Fluorescence of microtubules

Future Directions

- Improving quality of microtubule preservation
- Refining indirect immunofluorescence staining techniques
- Improving the strength of fluorophores
- Micromanipulation to assess force measurements [1]
- Greater cell viability during live cell imaging

References

1. Lin, N.K., Nance, R., Szybist, J., Cheville, A., Paliulis, L.V. Micromanipulation of Chromosomes in Insect Spermatocytes. J. Vis. Exp. (140), e57359, doi:10.3791/57359 (2018).

2. Nicklas RB. How cells get the right chromosomes. Science. 1997 Jan 31;275(5300):632-7. doi: 10.1126/science.275.5300.632. PMID: 9005842.

3. R.B. Nicklas, P. Arana; Evolution and the meaning of metaphase. *J Cell Sci* 1 August 1992; 102 (4): 681–690. doi: https://doi.org/10.1242/jcs.102.4.681

Acknowledgements

We thank Bucknell Professor of Biology Dr. Leocadia Paliulis, Bucknell Biology graduate student Ashley Borseth, and the Bucknell Biology Department for the funding necessary to conduct this research.

Risk of Thoracic Aortic Aneurysm Increased by Pathogenic Variants in TGFβ Signaling Pathway

Hannah Mirshahi, Jeremy S. Haley, MS, Diane T. Smelser, PhD, David J. Carey, PhD

Geisinger

Abstract

Deaths caused by thoracic aortic dissections and ruptures are preventable through surgical repair of aortic aneurysms. Previous work has demonstrated genetic factors to play a role in aneurysms. Identifying genetic variants that put individuals at risk can help provide early preventative measures. Using exome and clinical data from the MyCode cohort, we identified several variants in the TGFβ signaling pathway that may increase risk of TAA. Future studies of these variants and this pathway can provide early detection of aneurysms and provide insight into the disease mechanism.

Genetic Basis of Thoracic Aortic Aneurysms (TAA)

- TAAs occur when enlargement of aorta leads to aortic wall tear, allowing blood flow to separate wall layers and cause rupture of aorta
- Autosomal dominant mode of inheritance
- Enrichment of cases in males, those over 55 years of age, smokers

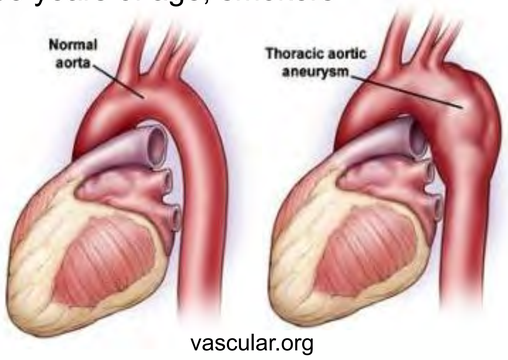

vascular.org

TGFβ Signal Pathway Plays Role in Maintaining Vascular Integrity

- Canonical TGFβ signals are essential for contractile unit maintenance in aortic smooth muscle cells
- Pathogenic variants in *SMAD3*, *TGFB2*, *TGFBR1*, *TGFBR2* genes are predicted to reduce intracellular kinase activity of TGFβ receptors

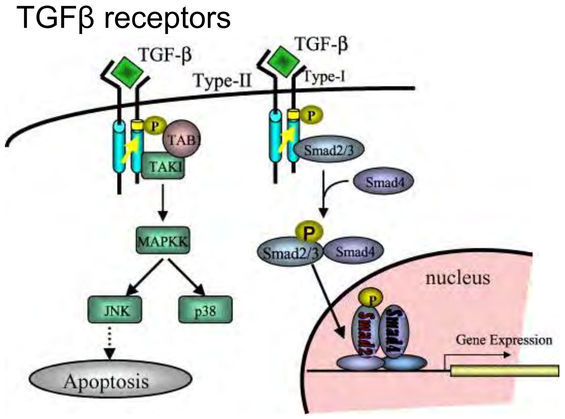

Journal of Dermatological Science

Methods

- Used exome sequencing data from the MyCode cohort to identify variants in TGFβ pathway
- Annotated variants using RefSeq and assigned pathogenicity interpretations based on ClinVar
- International Classification of Disease 9/10 used to identify cases
- Risks calculated using odds ratios (95% CI) and modeled through forest plots
- This study has been reviewed by the Geisinger Internal Review Board

Prevalence and Consequence of Variants in TGFβ Pathway Genes

Gene	Novel PTV	Novel MIS	VUS	PATH	PTV
SMAD3	2 (3)	56 (148)	39 (214)	4 (10)	7 (9)
TGFB2	3 (5)	76 (117)	31 (2081)	3 (3)	5 (7)
TGFBR1	8 (17)	82 (152)	56 (1139)	2 (2)	10 (19)
TGFBR2	8 (59)	82 (116)	87 (2055)	3 (5)	9 (61)

Variants (# Carriers)
VUS – Variants of Uncertain Significance
PATH – ClinVar Pathogenic Variants

Prevalence of TAA Among Pathogenic Variant Carriers

SMAD3	TGFB2	TGFBR1	TGFBR2	Aggregate
1 in 5	1 in 3	1 in 2	1 in 5	1 in 4

Individual Variant Inheritance in Families

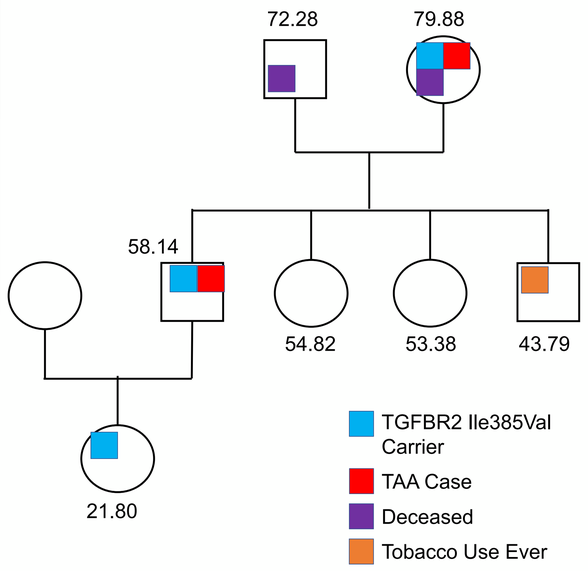

Pathogenic and Protein-Truncating Variants in *SMAD3*, *TGFB2*, *TGFBR1*, *TGFBR2* Genes Increase Risk of TAA

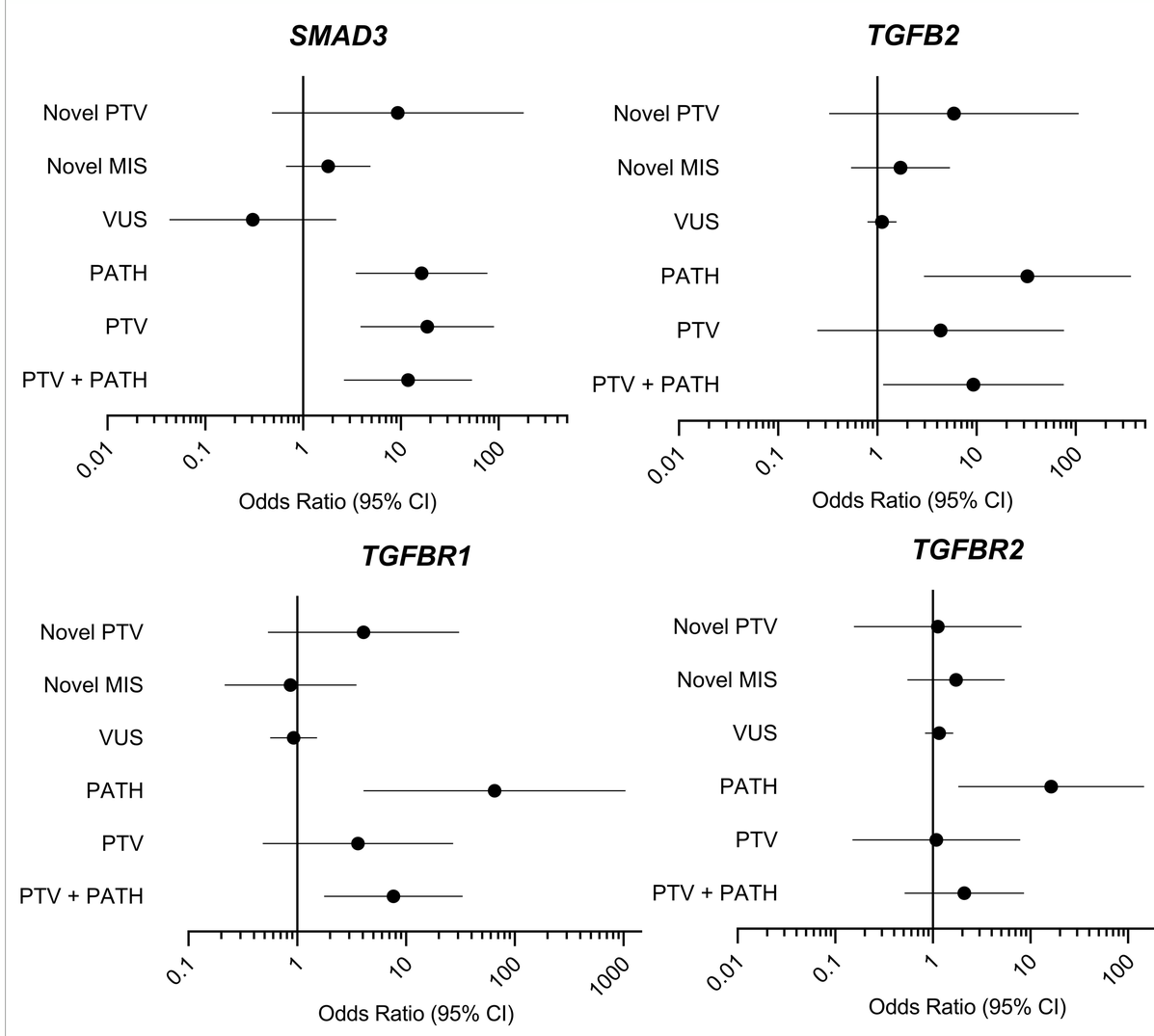

Discussion

- Large cohorts that combine genetic and clinical data enable assessment of genetic risk for disease
- Use of MyCode data enabled us to identify novel genetic risk factors for TAA in TGFβ pathway
- These data can guide improved care by early identification of patients who are at higher risk of TAA
- Knowledge of genetic factors in TGFβ pathway that affect TAA risk can provide mechanistic insight and potential novel therapeutic targets for treatment of TAA

Summary

- Identified hundreds of missense and protein-truncating variants in four major genes in TGFβ pathway
- Classified variants based on pathogenicity and identified pathogenic variants in each gene
- Using clinical data and pedigrees, determined that some variants increase risk of TAA

Future Directions

- Monitor charts of pathogenic variant carriers for any signs of disease progression
- Investigate variants affecting SMC contraction and adhesion to cellular

Acknowledgements

- The Carey Group, Geisinger Dept of Molecular and Functional Genomics
- Geisinger SURP Program

References

Pinard A, Jones GT, Milewicz DM. Genetics of Thoracic and Abdominal Aortic Diseases. Circ Res. 2019 Feb 15;124(4):588-606
Carey DJ et al. The Geisinger MyCode community health initiative: an electronic health record-linked biobank for precision medicine research. Genet Med. 2016 Sep;18(9):906-13. doi: 10.1038/gim.2015.187. Epub 2016 Feb 11. PMID: 26866580; PMCID: PMC4981567.

Sex chromosome aneuploidies and risk of neuropsychiatric disorders in two population-based cohorts

List authors here: John Seibert[1]; Alexander Berry[1]; Matthew Oetjens[1]
[1]Geisinger Medical Center, Danville, PA

Introduction

- Individuals with sex chromosome aneuploidies, characterized by an atypical number of X or Y chromosomes, collectively comprise a common but under-diagnosed genetic group, with prevalence estimates ranging from 1 in 1400 births to 1 in 650 births.

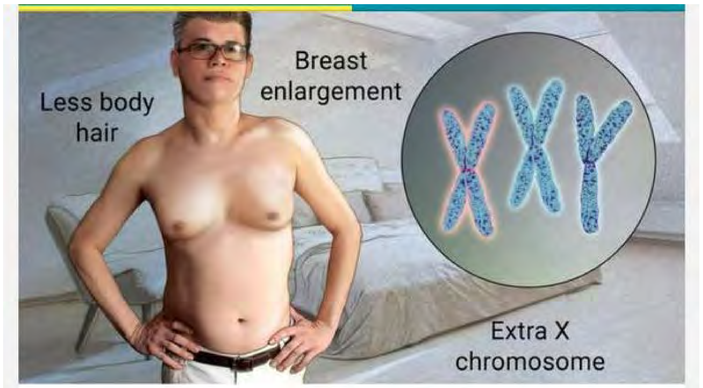

. Image from https://www.mayoclinic.org/

Figure 1: Clinical features of Klinefelter syndrome

- Individuals with sex chromosome aneuploidies are reported to be at increased risk for neuropsychiatric disorders (NPD). However, this association is not well characterized.

- We leveraged two large population-based cohorts with linked genetic and health data to investigate the relationship between sex chromosome aneuploidy and NPD.

- MyCode, Geisinger's biobank, analyzes consenting patients' DNA and returns clinically actionable findings to them.

- The All of Us research program aims to make advances in tailoring medical care to the individual. Its mission is to accelerate health and medical breakthroughs, enabling individualized prevention, treatment and care.

Materials and Methods

- To assess the frequency of relevant neuropsychiatric disorders, the International Classification of Diseases, Ninth Revision and International Statistical Classification of Diseases and Related Health Problems, Tenth Revision billing codes were extracted from linked EHRs as described Martin et al. 2020.

- Age was calculated based on the last encounter in EHR. Tests of association were per- formed with logistic regression adjusted for age and sex. Re- ported P values were 2-sided.

- Sex chromosome aneuploidies were called in MyCode using the protocol reported by Oetjens et al. 2019. In this study, we included four sex chromosome aneuploidies 47,XXY (Klinefelter syndrome); 47, XXX (trisomy X syndrome); 47, XYY (47,XYY syndrome) and 45,X (Turner syndrome).

Results

- Among the most common NPD diagnoses in MyCode, they consisted of anxiety and depression. This finding is similar in the All of Us cohort as well.

Table 1: Prevalence of NPD in MyCode and AllofUs

	MyCode			AllofUs		
NPD	**Controls**	**Cases**	**%**	**Controls**	**Cases**	**%**
ID	170,563	2,208	1.29	98,455	167	0.35
EP	166,360	6,411	3.85	96,792	1,830	3.88
ADHD	166,384	6,387	3.84	97,021	1,601	3.40
ANX	113,724	59,047	51.92	82,202	16,420	34.8
BPD	164,728	8,043	4.88	92,701	5921	12.6
DEP	126,322	46,449	36.77	81,740	16882	35.8
SLP	171,404	1,367	0.80	98,356	266	0.56
SCZ	168,798	3,973	2.35	96,668	1954	4.15
OCD	170,803	1,968	1.15	98,085	537	1.14
COM	169,989	2,782	1.64	98,366	256	0.54
CP	171,356	1,415	0.83	98,540	82	0.17
Motor	171,637	1,134	0.66	97,644	978	2.07
ASD	171,459	1,312	0.77	98,511	111	0.24
OND	172,713	58	0.03	98,510	112	0.24

ID: Intellectual Disability; CD: Communication Disorder; ASD: Autism Spectrum Disorder; ADHD: Attention Deficit and Hyperactivity Disorder; SLD: Specific Language Disorder; MD: Motor Disorder; OND: Other Neurodevelopmental Disorder; SCZ: Schizophrenia and Related Disorder; BPD: Bipolar Disorder; OCD: Obsessive Compulsive Disorder; EP: Epilepsy; CP: Cerebral Palsy;

- The most-rare diagnoses in MyCode are autism, motor disorders, and other neurological disorders. In the All of Us cohort, the most rare diagnoses are cerebral palsy, autism, and other neurological disorders.

- The most common disorders were similar between the All of Us and MyCode cohorts. The rarest disorders were differing, with cerebral palsy in All of Us and motor disorders being in MyCode.

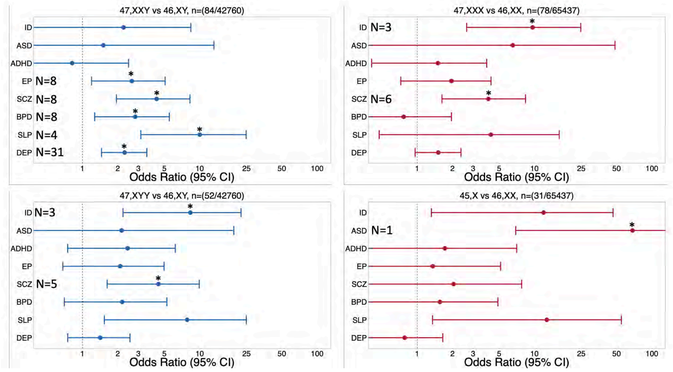

Figure 2: Risk of NPD in patients with sex chromosome aneuploidies in MyCode

- In MyCode, sex chromosome aneuploidies increased risk of NPD between 5-10x higher compared to individuals with a typical sex chromosome complement

Discussion

- Overall, the prevalence for NPD diagnoses were similar between the MyCode and All of Us cohorts. This was displayed through the proportion of cases.
- Individuals with sex chromosome aneuploidies are at an increased risk of NPDs.

References

C. L. Martin, *et al.*, Identification of Neuropsychiatric Copy Number Variants in a Health Care System Population. *JAMA Psychiatry* (2020)

M. T. Oetjens, M. A. Kelly, A. C. Sturm, C. L. Martin, D. H. Ledbetter, Quantifying the polygenic contribution to variable expressivity in eleven rare genetic disorders. *Nat. Commun.* **10**, 4897 (2019).

Data sharing between Get-2-Goal medical app and Apple Health app

Claire Engel

Bucknell University
Computer Science Department
2022

INTRODUCTION

- The Get 2 Goal project is a joint collaboration between the CS department (with Prof Lea Wittie), the Geisinger Obesity Institute (GOI) (with Dr Chris Still and Dr Lisa Bailey-Davis) and Bucknell undergraduates.
- Students create apps for phones and web browsers with formulas published by the GOI that guide doctors and patients in making decisions about whether to perform bariatric surgery and track the recovery process after surgery.

My task focuses on implementing Apple's HealthKit and ResearchKit. HealthKit allows for the sharing of weight data between different iOS apps through the Apple Health app. ResearchKit will allow us to collect data from the users, including how often they open the app, any settings they change, and any information they enter into the app to evaluate the app's usage.

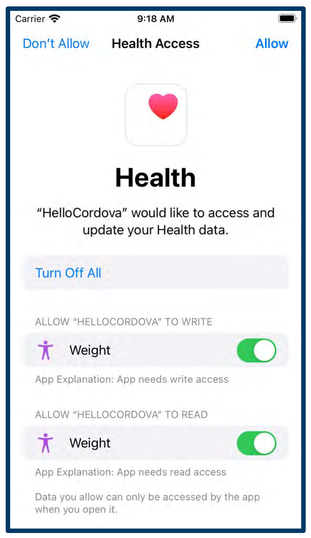

Figure 1. Permission screen created by HealthKit that pops up when permission is requested

DATA FLOW

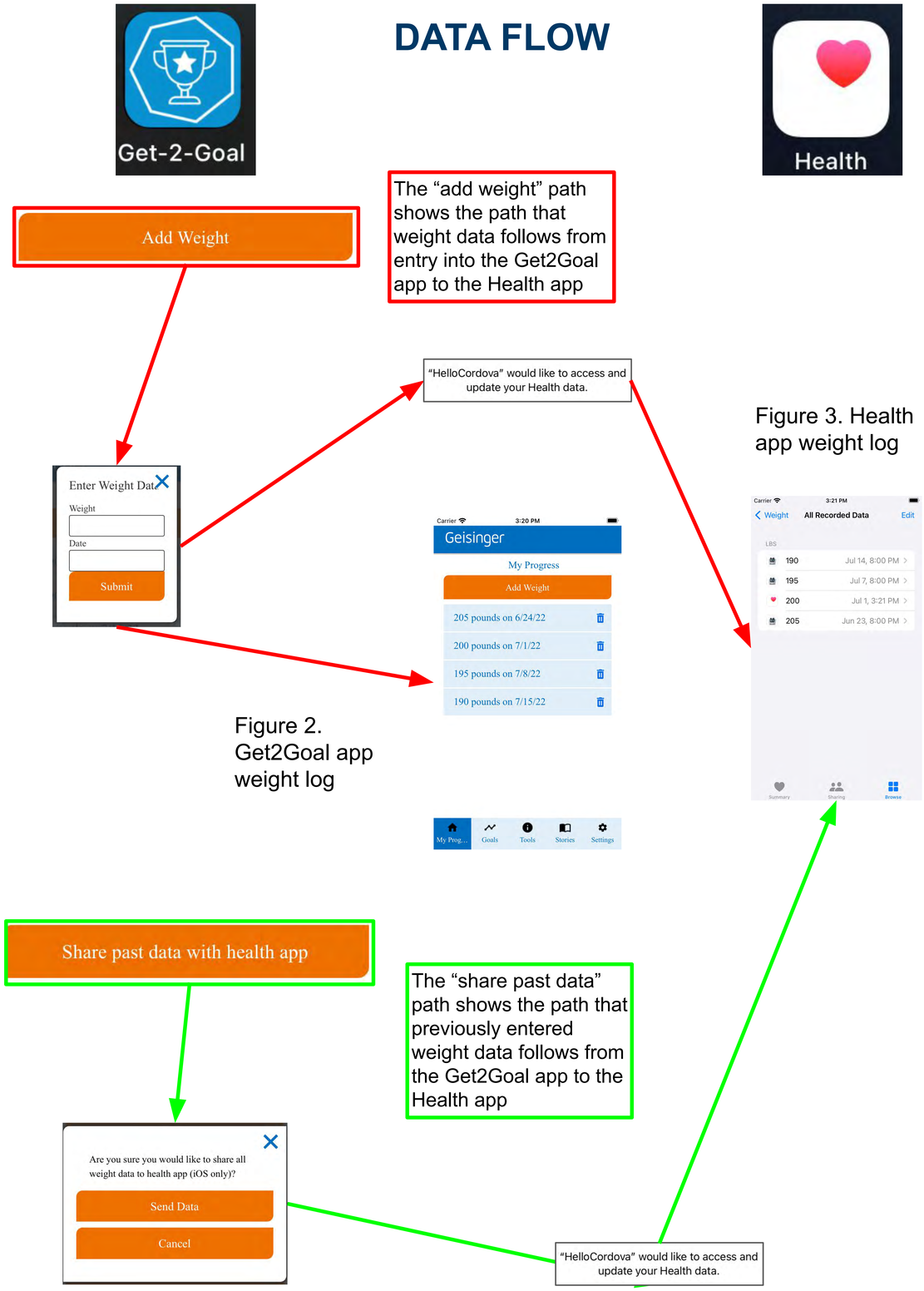

Figure 2. Get2Goal app weight log

Figure 3. Health app weight log

APPROACH

- Learned languages: Javascript, HTML, CSS
- Reviewed existing app code (Javascript, HTML, CSS) and existing HealthKit code (Swift, Objective-C)
- Installed software for the ability to emulate the app on a computer

SAMPLE FUNCTION

```
function add_data() {
    if (window.cordova.platformId == "ios") {
        var weight = document.getElementById("weightEntry").value;
        var date = new Date(document.getElementById("dateEntry").value);
        window.plugins.healthkit.saveWeight(
            { 'unit': 'lb', 'amount': weight, 'date': date },
            function() {
                var weight = document.getElementById("weightEntry").value;
                var date = document.getElementById("dateEntry");
                if(weight != "") {
                    window.plugins.healthkit.saveQuantitySample( {
                        "sampleType": "HKQuantityTypeIdentifierWeight",
                        "startDate": date,
                        "endDate": date,
                        "unit": "lb",
                        "amount": weight
                        } );
...
```

- Uses HealthKit functions to send weight data from Get2Goal to Health
- Takes weight and date from "Add Weight" popup entry window
- Saves the given weight as a quantity sample in Health

FUTURE CONSIDERATIONS

Retrieve weight data from health app

- ResearchKit
  - Allows data to be collected from app users for research purposes
- Health and research integration for android

REFERENCES

1. https://www.researchandcare.org/researchkit/
2. https://developer.apple.com/health-fitness/

Genetic Basis of Long QT Syndrome through Analysis of MyCode Patient Data

Yahya M. Khan, Cassandra M. Hartle, Tooraj Mirshahi
Dept. Molecular and Functional Genomics
Geisinger, Danville, PA

Background

- Long QT Syndrome is a genetic disorder that can cause sudden cardiac death: it is an arrythmia of the ventricles.
- A hallmark of LQTS is an elongated corrected QT (QTc) interval on the ECG

Electrocardiogram: Long QT Syndrome

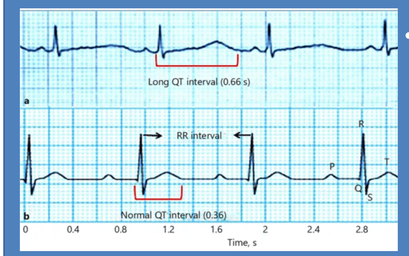

- QTc is the QT interval corrected for heart rate

- Caused by mutations in one of 17 genes: *KCNQ1, KCNH2, SCN5A, AKAP9, CACNA1C, CAV3, KCNE1, KCNE2, KCNJ5, SCN4B, SNTA1, ANKB, KCNJ2, CALM1, CALM2*
- LQTS is rare: 1/2000 people affected

Prevalence of LQT Syndromes

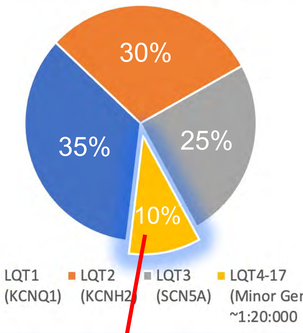

Goal: Use MyCode cohort to determine the prevalence of LQTS caused by minor genes

Approach: Study 6 genes where loss of function variants should cause a phenotype: ***AKAP9, KCNE2, KCNJ5, ANKB, KCNE1, KCNJ2***

Methods

- Identify truncating variants in 6 genes of interest
- Identify individuals carrying these variants
- Calculate QTc intervals from ECGs in the electronic health records (EHR)
- Find ICD codes for LQTS from EHR
- Determine whether truncating variant carriers in these genes have LQTS

Results from 6 Genes of Interest

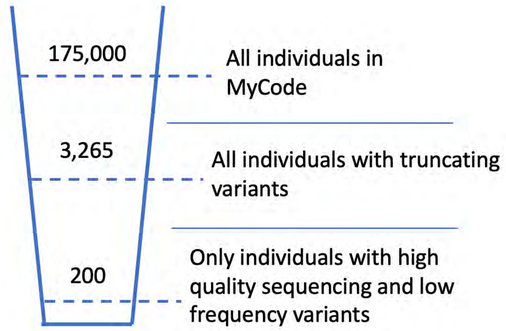

It is not possible that all 200 protein truncating variants are LQTS. We expect ~10 people to have LQTS via minor genes.

Conclusions:

- Any given minor gene may not be an LQTS gene
- Loss of function may not be not causal of LQTS
- Loss of function may have low penetrance

In Depth Examination:

KCNJ2 is a minor gene that is actively being studied in this lab. KCNJ2 patients will be examined to see if individuals with truncating variants have LQTS.

- QTc is one way of determining patients that may have LQTS, however, QTc changes with age. QTc's should be compared in the context of age to evaluate elongation:

Average QTc vs. Age Range of MyCode Patients

Average QTC	Age Range
425	0 to 10
423	10 to 20
424	20 to 30
432	30 to 40
435	40 to 50
437	50 to 60
440	60 to 70
444	70 to 80
448	80 to 90
450	90 to 100

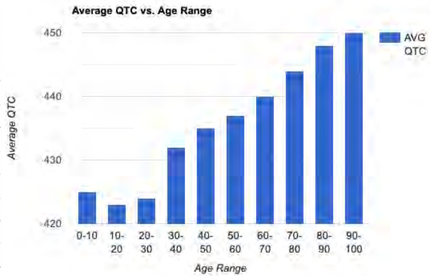

- Average QTc's per age range serves as age-matched control
- Used to evaluate QTc elongation for KCNJ2 patients

- QTc alone is not the best way of evaluating LQTS presence. Confounding factors may be causing an elongated QTc:

Protein Truncating KCNJ2 variants

Patient	Mutation	Consequence	Age	Number of ECGs	Average QTc	Confounding Factors
1	Arg40Ter	stop_gained	60	1	523	None, only had one ECG
2	Arg40Ter	stop_gained	72.7	4	453	--
3	Arg40Ter	stop_gained	58	4	434	--
4	Arg40Ter	stop_gained	39.1	2	430	--
5	Arg40Ter	stop_gained	90.5	2	499	Significant age, coronary atherosclerosis, vascular disease, heart failure, only 2 ECGs
6	Arg40Ter	stop_gained	58.4	4	423	--
7	Glu118Ter	stop_gained	88.9	25	487	Significant age, heart failure, atrial fibrillation
8	Leu368fs	frameshift	76.7	16	427	--
9	Glu241fs	frameshift	37	0	--	--

- Three patients had elongated QTc's that were compared to age-matched control
- Patients 5 and 7 had elongated QTc's, but investigation of ICD codes and age presented confounding factors that make LQTS unlikely

Summary:

- Three total individuals were found to be likely candidates for LQTS from minor genes
- Protein truncating variants on KCNJ2 did not cause LQTS
- Cases of elongated QTc's had confounding factors

Conclusion:

- The presence of a mutation in genotype does not necessarily mean that a phenotype will be expressed
- Loss of function may not be causal of LQTS or it has a low penetrance
- Phenotypic expression depends on the type of mutation and where it occurs in the amino acid sequence

References

Behzadi, M. et. al. (2018). Opioids and Cardiac Arrhythmia: A Literature Review. Medical principles and practice : international journal of the Kuwait University, Health Science Centre, 27(5), 401–414. https://doi.org/10.1159/000492616

Giudicessi, J. R., & Ackerman, M. J. (2013). Genotype- and phenotype-guided management of congenital long QT syndrome. Current problems in cardiology, 38(10), 417–455. https://doi.org/10.1016/j.cpcardiol.2013.08.001

Funding

This project was funded by Geisinger Clinic to TM.

Accessibility - Get2Goal Medical App

Omid Mohammadi

Bucknell University
Computer Science Department
2022

INTRODUCTION

- The Get 2 Goal project is a joint collaboration between Bucknell CS department, Geisinger Obesity Institute, and Bucknell undergraduates.
- Obesity is a disorder involving excessive body fat that increases the risk of health problems. According to the Center for Disease Control (CDC), approximately 36.9% of American adults age 20 and older were obese based on 2015-2016 data.
- United States counts around 61 million adults with disabilities. That represents 26% of adults in the US or 1 in 4 adults.

My task focuses on implementing accessibility guidelines throughout the Get2Goal application and website page to ensure that all people can perceive, understand, navigate, and interact with its content regardless of their disability. Whether it is a physical, cognitive, hearing or visual impairment, disabilities can make interacting with a desktop or mobile phone very difficult and challenging.

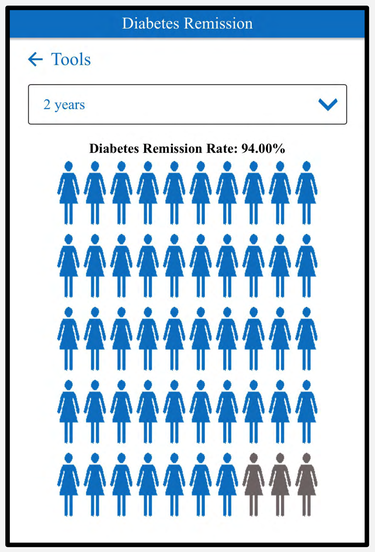

Figure 1. Screenshot showing 2-year diabetes remission among bariatric surgery patients based on patient demographics.

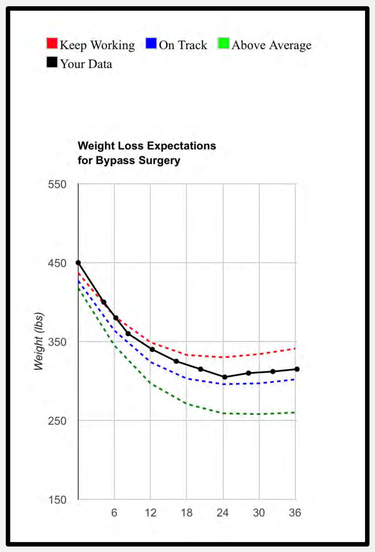

Figure 2. Screenshot showing the goals graph page of G2G app, tracking weight loss after surgery.

RESULTS

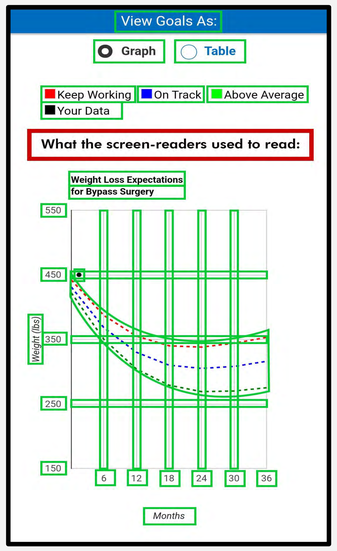

Figure 3. Screenshot showing that screen-readers used to read unnecessary elements on graphs and charts.

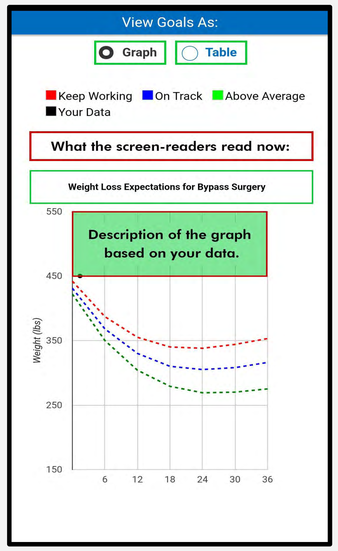

Figure 4. Screenshot showing the updated version of the G2G app, which describes the graph to the screen-readers.

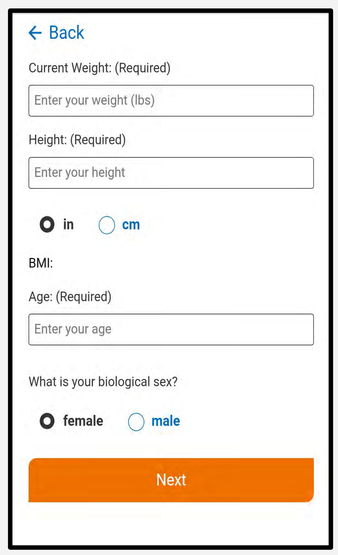

Figure 5. Screenshot showing the onboarding page of Get2Goal app with the new design implemented.

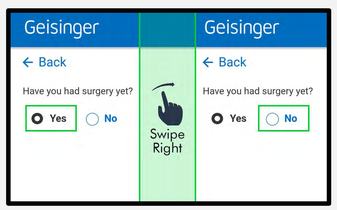

Figure 6. Screenshot showing screen-reader traversing in a correct order.

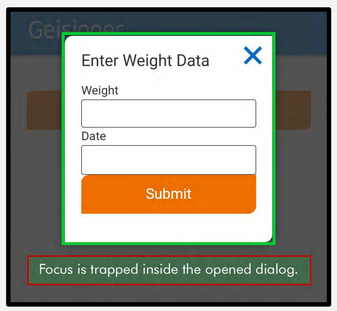

Figure 7. Screenshot showing focus is trapped inside the opened dialog, where previously the screen-reader would have gone through background elements.

APPROACH

- Studied Web Content Accessibility Guidelines (WCAG) international standard.
- Learned Languages: JavaScript, HTML, and CSS.
- Ran accessibility tests on Get2Goal app and website.
- Presented at weekly interdisciplinary team meetings with Geisinger Obesity Institute and Bucknell CS Department.
- Attended research interviews conducted by prof. Anne Ross, with accessibility experts.

SUMMARY

- Assesed the accessibility features of Get2Goal application and website.
- Implemented accessibility guidelines throughout the application.
- Redesigned parts of the Get2Goal application to create a better user experience.
- Added descriptions for all the graphs and charts in the application.
- Wrote functions to help with the flow of the application and improve accessibility.

FUTURE CONSIDERATIONS

- Create custom controls to change the properties of Get2Goal application such as font size changes to increase the readability.
- Apply accessibility features to the Get2Goal website.

REFERENCES

1. MDN Web Docs. Accessibility. Website.
2. Web Accessibility Initiative (WAI). Aria authoring practice guide. Website.
3. The A11Y Project. WCAG Compliance. Website.
4. Centers for Disease Control and Prevention. (2020, September 16). Disability impacts all of us infographic.

Predicting Patient-Specific Optimal Deep Brain Stimulation Locus Using Subthalamic Nucleus Anatomy

Collin Murphy[1], Karlo A. Malaga Ph.D.[1]

1. Department of Biomedical Engineering, Bucknell University, Lewisburg, PA

Introduction

- Subthalamic nucleus (STN) is the standard target for deep brain stimulation (DBS) in treatment of Parkinson disease (PD)[1]
- Optimal stimulation location is seldom agreed upon in literature
- **Objective:** Determine relationship between STN anatomical features and patient-specific optimal stimulation location in PD patients, allowing physicians to predict DBS targeting from pre-op imaging

Methods

- Utilized 87 segmented PD patient STNs and associated stimulation parameters in DBS treatment from retrospective study[2]
- Volume, sphericity, and two metrics for flatness in the three anatomical views were generated for each STN model

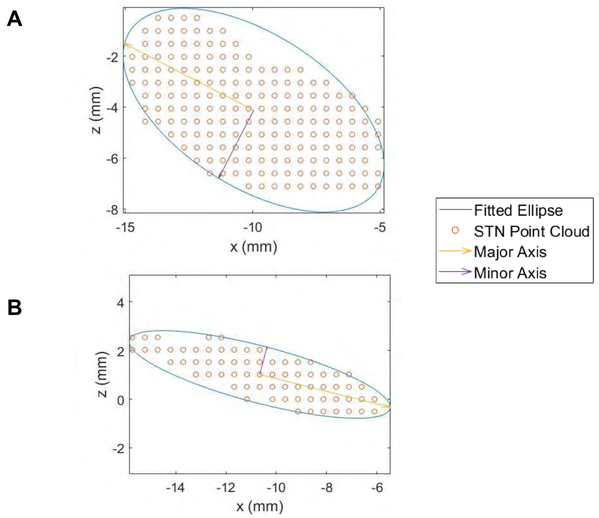

Fig. 1. Fitted ellipses used for flatness metrics. Ellipses fitted to 2D projections of patient STN point clouds. (A) Represents "fat" STN with respect to minor axis length. Axes are represented as purple and yellow vectors. (B) Represents "flat" STN with respect to minor axis length.

- Volume of tissue activated (VTA) was used to compute dorsal, ventral, medial, lateral, anterior, and posterior activation percentages
- Patients were grouped based on active contact location as well as VTA-based stimulation location in each of the three anatomical directions
- Wilcoxon rank sum and Kruskal Wallis tests were used to compare anatomical features among groups

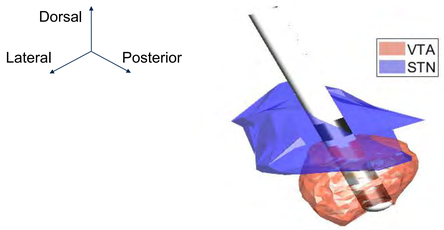

Fig. 2. Model of VTA-STN-Electrode Contact Overlap. VTA (orange) propagation from active contact (red) is modeled above relative to one patient's STN (blue).

Results

No significant differences in anatomical features in coronal or sagittal views between active contact groups (all directions)

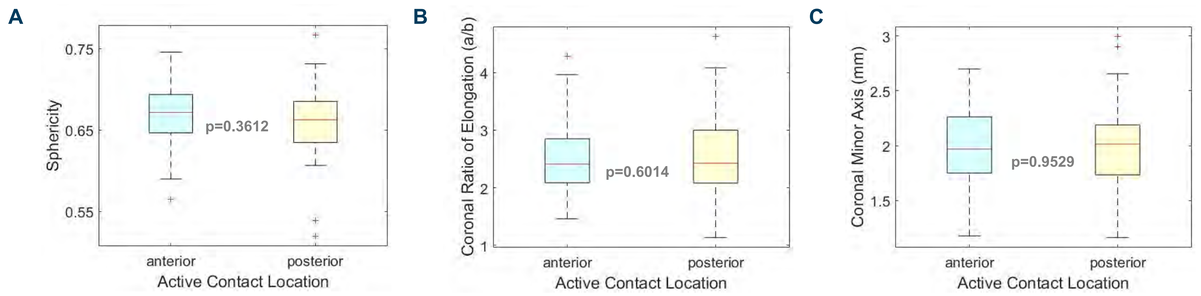

Fig. 3. Active contact grouping in y direction. Boxplot groups were generated based on active contact location relative to STN centroid. (A) Sphericity of patient STNs was compared using Wilcoxon rank sum test. No significant difference was found. (B) Ratio of STN major axis length to minor axis length (from ellipses in coronal projection) was compared using Wilcoxon rank sum test. No significant difference was found. (C) Minor axis length of STN (from ellipses in coronal projection) was compared using Wilcoxon rank sum test. No significant difference was found.

No significant differences in anatomical features between VTA-based stimulation groups (all directions)

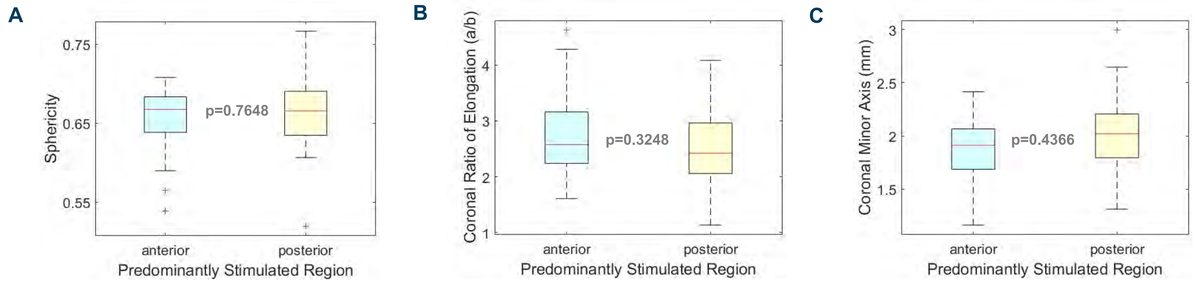

Fig. 4. VTA-based stimulation grouping in y direction. Boxplot groups were generated based on the ratio of posterior to anterior STN activation (posterior if ratio>1, anterior if ratio<1). (A) Sphericity of patient STNs was compared using Wilcoxon rank sum test. No significant difference was found. (B) Ratio of STN major axis length to minor axis length (from ellipses in coronal projection) was compared using Wilcoxon rank sum test. No significant difference was found. (C) Minor axis length of STN (from ellipses in coronal projection) was compared using Wilcoxon rank sum test. No significant difference was found.

Significant differences between flatness metrics in axial projection

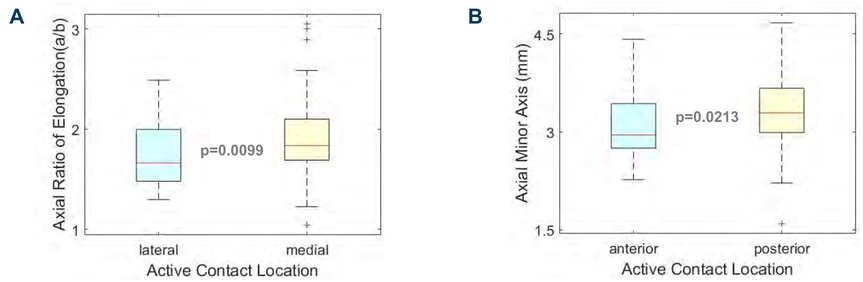

Fig. 5. Flatness metrics across active contact location grouping . Boxplot groups were generated based on active contact location relative to STN centroid. (A) STNs with medial active contacts were significantly rounder in an axial view (Wilcoxon rank sum test). The same trend was not observed when grouping by VTA-based stimulation. (B) STNs with anterior active contacts were significantly flatter in an axial view (Wilcoxon rank sum test). The same trend was not observed when grouping by VTA-based stimulation.

No significant difference in dorsal or posterior STN activation when grouping by active contact location

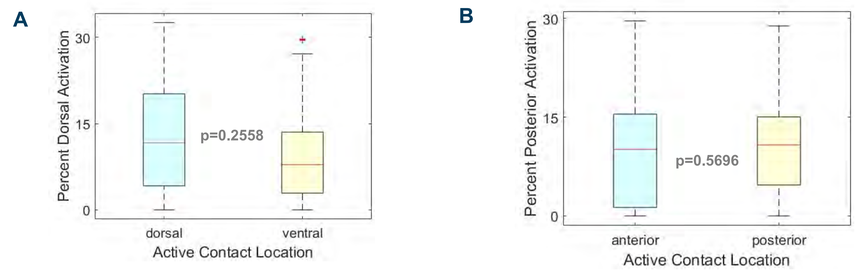

Fig. 6. Regional STN activation across associated active contact location grouping. Boxplot groups were generated based on active contact location relative to STN centroid. (A) No significant difference in dorsal activation between STNs with dorsal and ventral active contacts (Wilcoxon rank sum test). (B) No significant difference in posterior activation between STNs with anterior and posterior active contacts (Wilcoxon rank sum test).

Conclusion

- A significant difference was found in STN flatness metrics of the axial projection between groups based on active contact location
- Based on lack of significance in the same trends with VTA-based grouping, further evidence is necessary to suggest that any of the anatomical features analyzed are suitable predictors for therapeutic stimulation location
- The same differences were insignificant across VTA-based stimulation groups
- Concluded possible directional bias in spread of stimulation; compared regional activation across active contact location groups
- No significant difference in dorsal activation between dorsal and ventral active contacts (significant difference expected)
- No significant difference in posterior activation between anterior and posterior active contacts (significant difference expected)
- Further investigation should compare fractional anisotropy values between STN anatomical regions to explain directional bias in stimulation propagation

Acknowledgements

The authors would like to thank the patients involved in this study for their voluntary participation and Parag G. Patil, M.D., Ph.D., Kelvin L. Chou, M.D., Aidan Ahamparam, and Joseph T. Costello from the University of Michigan for clinical data and data visualization code.

This project is supported by the Emerging Scholars Program at Bucknell University.

References

1. Dembek, T. A., Roediger, J., Horn, A., Reker, P., Oehrn, C., Dafsari, H. S., Li, N., Kühn, A. A., Fink, G. R., Visser-Vandewalle, V., Barbe, M. T., & Timmermann, L. (2019). Probabilistic sweet spots predict motor outcome for deep brain stimulation in Parkinson disease. Annals of Neurology, 86(4), 527–538. https://doi.org/10.1002/ana.25567
2. Malaga, K. A., Costello, J. T., Chou, K. L., & Patil, P. G. (2021). Atlas-independent, N-of-1 tissue activation modeling to map optimal regions of subthalamic deep brain stimulation for Parkinson disease. NeuroImage: Clinical, 29, 102518.

Contact Information

Computational Neuromodulation Lab
Department of Biomedical Engineering
Bucknell University, Lewisburg, PA

cpm017@bucknell.edu

Bacteria Impaired Streams In Union County

Melanie Gamboa

Faculty Advisors: Carley Gwin and Deborah Sills

Department of Civil and Environmental Engineering, Bucknell University, Lewisburg, Pa.

Goals

- Collaborate with Buffalo Creek Watershed Alliance (BCWA) to Identify specific streams in Union County which qualify as impaired, based on presence of harmful bacteria.
- Find possible correlations between water quality parameters

Background

Many of Pennsylvania's waterways are unfit for drinking, recreation, fishing, and aquatic life. According to Pennsylvania Code's water quality standards[1], Union County's impaired waterways are dangerous for human recreation which prohibits the residents in this county from having access to the water in their own backyard.

Figure 1. An impaired stream that is being used for recreation

Methods

1. Sample streams in Union county that have not met PA DEP standards for recreation in the past. Sample 13 sites 5 times within 30 days. Resulting in 71 samples.

Figures 2. & 3. Our team sampling impaired streams

2. Process water samples in Lab

Water quality parameters measured:

- pH
- Conductivity
- Temperature
- Dissolved Oxygen(D.O.)
- Turbidity
- Solids(TSS)
- E.coli Coliforms
- Bacteria Coliforms
- DNA filtration

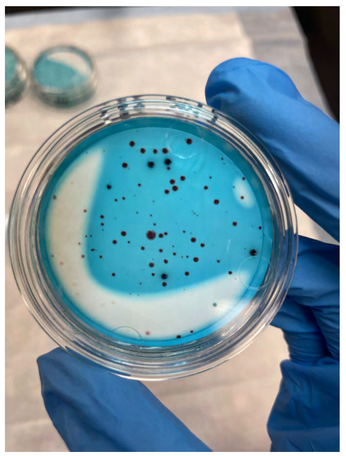

Figure 4. bacteria plate. Red coliforms represent bacteria in the water sample. Blue coliforms represent E.coli

mjg032@Bucknell.edu

Results

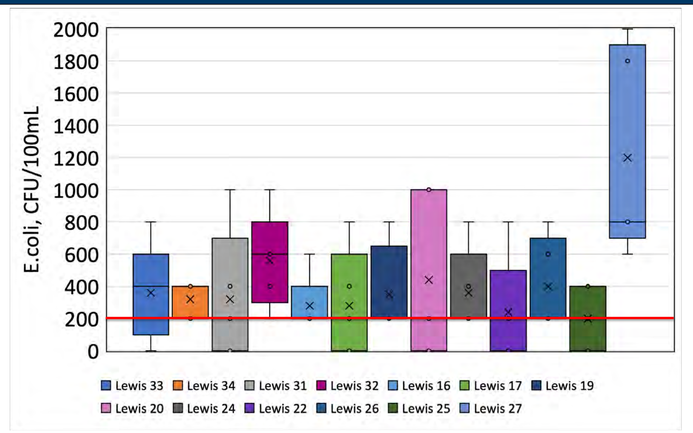

Figure 5. Measured E.coli coliforms in each site throughout the 5 sample days.

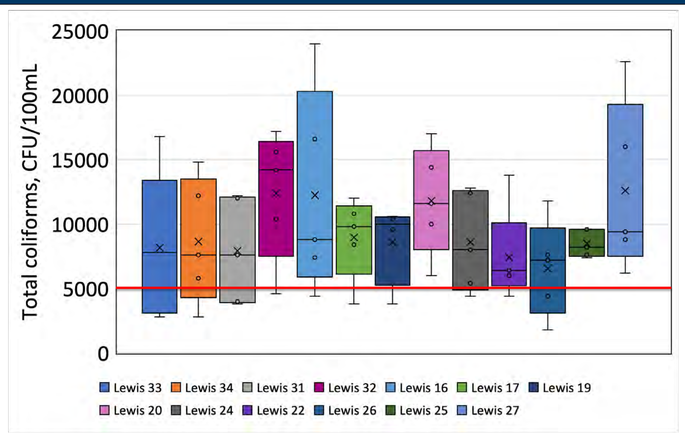

Figure 6. Measured total bacterial coliforms in each site throughout the 5 sample days.

Figures 5 and 6 show high amounts of bacteria and E.coli in streams across Union County. Many of these sites are in people's backyard where families use the streams for recreation. The PA DEP states that E.coli numbers should not reach 200 colony forming units per 100 mL (CFU/100 mL). As for total coliforms, waterways should not surpass 5,000 CFU/100mL.[1] BCWA hopes to use these results to convince county agencies to take action and limit pollutants from entering waterways.

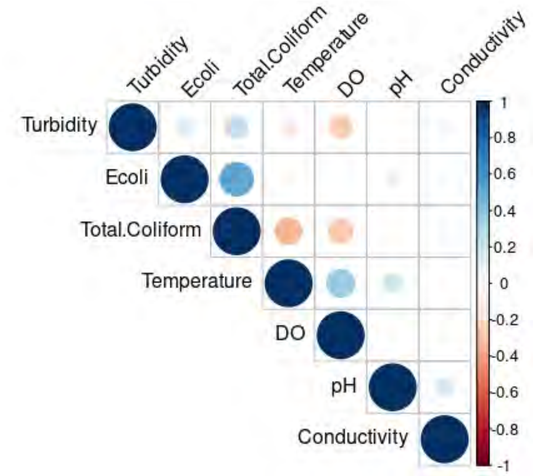

Figure 7. A correlation matrix of water quality parameters tested for of all 71 samples

Figure 7 shows that there are positive correlations between

1. E.coli and Turbidity
2. Total coliforms and turbidity
3. E.coli and Total Coliform
4. Temperature and D.O.
5. Temperature and pH
6. pH and conductivity
7. Total coliform and conductivity
8. pH and E.coli

Figure 7 shows that there are negative correlations between

1. Temperature and turbidity
2. D.O. and turbidity
3. Temperature and total coliform
4. D.O. and total coliforms
5. Temperature and E.coli
6. Conductivity and turbidity
7. D.O. and conductivity
8. D.O. and pH

Future Work

Where do the bacteria come from?

We will use Microbial Source Tracking[2] using DNA and qPCR tests to identify specific fecal polluters to these waterways

Figure 8. Microbial Source Tracking to Identify Fecal Pollution Sources in Water

Correlation Matrix

We will keep working with our correlation matrix to weed out outliers and create a more detailed figure to better understand correlations.

References

1. The Pennsylvania Bulletin webpage for the 2000 Water Quality Regulatory Basics Initiative Triennial Review rulemaking (https://www.pabulletin.com/secure/data/vol30/30-47/2027.html)
2. Elisenda Ballesté. "Implementation and integration of microbial source tracking in a river watershed monitoring plan." Science of The Total Environment. https://www.sciencedirect.com/science/article/pii/S0048969720330904.

Acknowledgements

The Civil and Environmental Engineering department and the Civic Engagement office for funds.
The Buffalo Creek Watershed Alliance for Sampling help and guidance.

Deep Brain Stimulation of the Subthalamic Nucleus and its Effect on Gait Disturbances in Parkinson Disease

Jacqueline Zak[1], Karlo A. Malaga[1]

1. Department of Biomedical Engineering, Bucknell University, Lewisburg, PA

Introduction

Although the standard target of deep brain stimulation (DBS) for Parkinson disease (PD) is the subthalamic nucleus (STN)[1], better outcomes may be obtained by stimulating regions within and around the STN, as this generalized approach may not be optimal for every patient due to the diversity of their symptoms

Objective: Identify the ideal stimulation spot within or around the STN to treat gait disturbances in PD with DBS using the volume of tissue activation (VTA) and compare to a traditional electrode contact analysis

Methods

- Utilized patient-specific imaging data from a retrospective study of 40 PD patients with 72 implantation sites
- An optimal stimulation location for treating motor symptoms was determined using tissue activation models [2]
- The VTA was used to quantify STN and non-STN activation in the lateral-medial, anterior-posterior, and dorsal-ventral directions
- Evaluated relationships between STN activation and symptom improvement, calculated from the Movement Disorder Society Unified Parkinson's Disease Rating Scale (MDS-UPDRS), items 3.10-3.12[3]
- Patients were grouped based on where most of the VTA-STN overlap was located relative to the STN centroid
- Symptom improvement between groups was compared with significance defined at $p < 0.05$ following corrections
- Electrode position (relative to the STN) was also examined for comparison

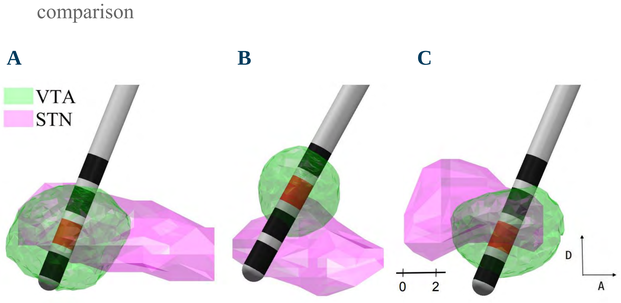

Figure 1. VTA-STN overlap. Sagittal view of the VTA (green) and STN (pink) boundary overlap for three patients. The DBS lead is shown with the active contact in red. VTA location variability is shown (A) posterior VTA, (B) centered VTA, (C) anterior VTA. STN activation corresponds to the overlapped green and pink area, external activation corresponds to the remaining green area. A: anterior; D: dorsal. Scale bar is shown in millimeters.

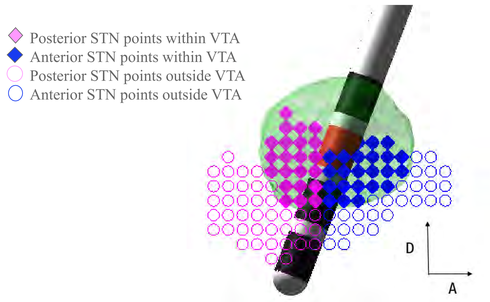

Figure 2. VTA anterior-posterior STN overlap. Sagittal view of VTA (green) and the electrode with the active contact (red) modeled for one patient. The STN points are displayed in either pink (posterior) or blue (anterior) the filled in points are ones which overlap with the VTA (activated STN points) and the open circles are points which do not overlap with the VTA (non-activated STN points).

Results

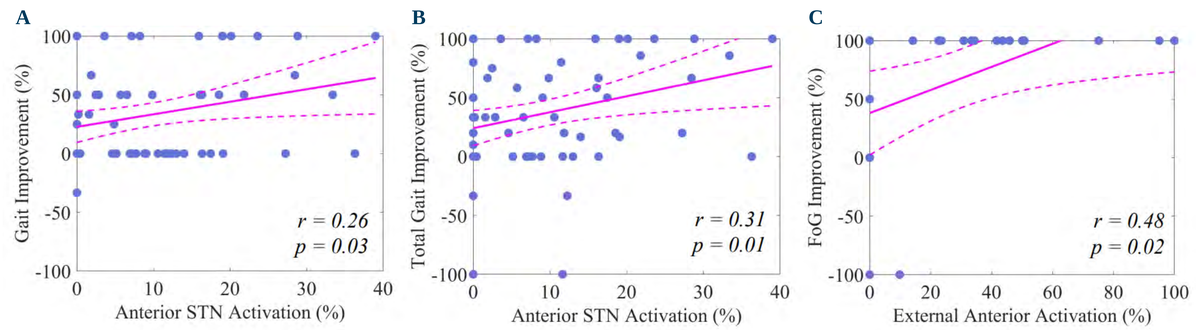

Figure 3. Linear regressions comparing VTA location and gait outcomes. (A) Relationship between anterior STN activation and gait improvement from stepwise regression analysis. (B) Relationship between anterior STN activation and total gait improvement from stepwise regression analysis. (C) Relationship between anterior external activation and freezing of gait (FoG) improvement. The linear fitted line (solid) and 95% confidence intervals (dashed) are shown in pink.

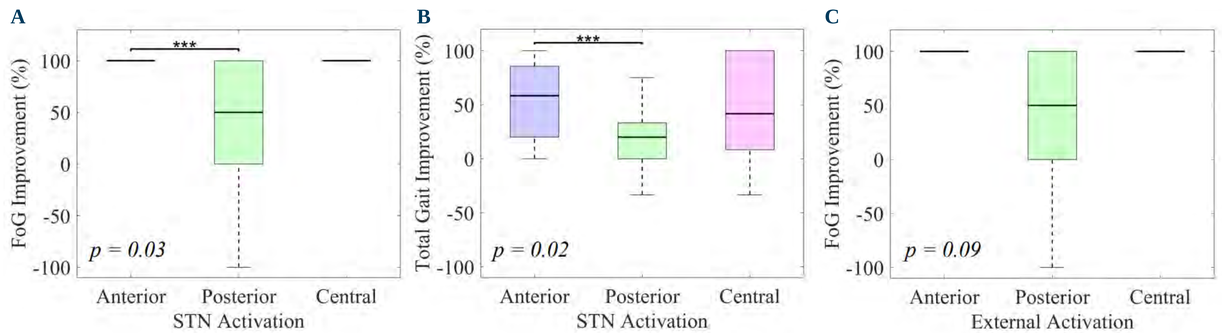

Figure 4. Kruskal-Wallis tests comparing VTA location and gait outcomes. (A) Box plot comparing majority anterior STN activation (n = 7) and majority posterior STN activation (n = 8) with respect to FoG improvement. The excluded central STN activation group (n = 4) is also shown. (B) Box plot comparing majority anterior STN activation (n = 22) and majority posterior STN activation (n = 19) with respect to total gait improvement. The excluded central activation group (n = 12) is also shown. (C) Box plot comparing majority anterior external activation (n = 7) and majority posterior external activation (n = 11) with respect to FoG improvement. The excluded central external activation group (n = 4) is also shown.

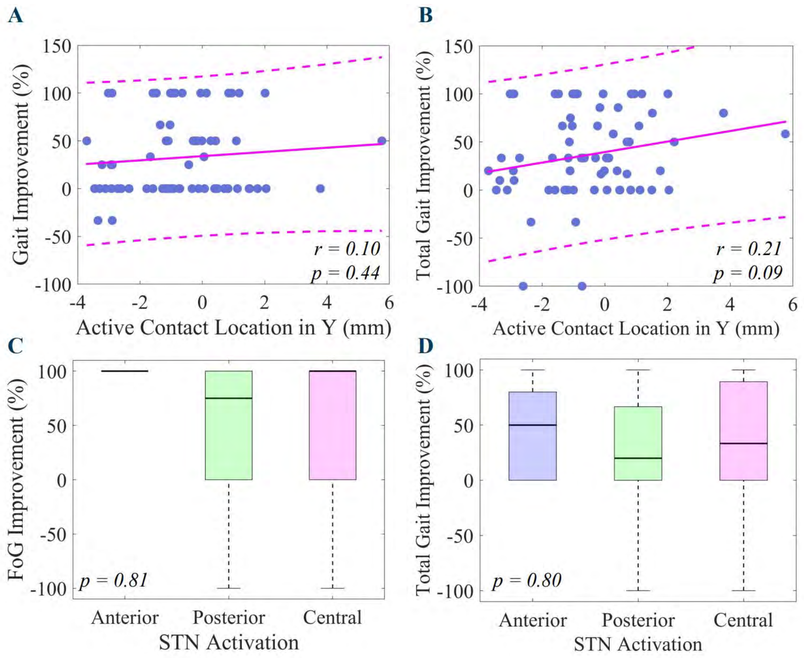

Figure 5. Paralleled electrode active contact analysis. (A) Relationship between active contact location in the y direction and gait improvement from stepwise regression analysis. (B) Relationship between active contact location in the y direction and total gait improvement from stepwise regression analysis. The linear fitted line (solid) and 95% confidence intervals (dashed) are shown in pink. (C) Box plot comparing anterior STN electrodes (n = 8) and posterior STN electrodes (n = 10) with respect to FoG improvement. The excluded central electrode group (n = 4) is also shown. (D) Box plot comparing anterior STN electrodes (n = 25) and posterior STN electrodes (n = 27) with respect to total gait improvement. The excluded central electrode group (n = 13) is also shown.

Conclusion

- A significant positive relationship was found between both anterior STN activation and gait improvement and between anterior STN activation and total gait improvement
- A significant relationship between anterior external activation and FoG improvement was also found despite most patients having complete improvement
- A significant difference between majority anterior and majority posterior STN activation was found for both FoG and total gait
- No relationship was found between gait disturbance improvement and electrode position

More anterior STN stimulation may be preferable to more posterior STN stimulation for patients whose primary symptoms are gait disturbances

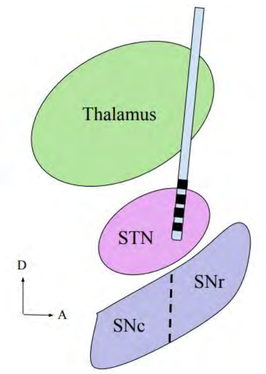

Figure 6. Anatomical relationships between STN and surrounding structures. The substantia nigra pars reticulata (SNr) may be a superior target for FoG specifically, as it is slightly anterior to the STN and located immediately adjacent.

Acknowledgements

The authors thank the patients involved in this study for their voluntary participation and Parag G. Patil, M.D., Ph.D., Kelvin L. Chou, M.D., Aidan Ahamparam, and Joseph T. Costello from the University of Michigan for clinical data and data visualization code.

This project was supported by the Emerging Scholars Program and the James L.D. and Rebecca Roser Research Fund at Bucknell University.

References

1. Dembek, T. A. et al., Ann. Neurol., 2019, 86(4), 527–538. https://doi.org/10.1002/ana.25567
2. Malaga, K. A., et al., NeuroImage: Clin., 2021, 29, 102518.https://doi.org/10.1016/j.nicl.2020.102518
3. Goetz, C. et al., J Mov Disord., 2008,1(414), 1–33.

Contact Information

Computational Neuromodulation Lab
Department of Biomedical Engineering
Bucknell University, Lewisburg, PA

jrz008@bucknell.edu